Chap.3 The nature of old Galactic components

- Overview of old Galactic components
  - bulge, thick/thin disks, stellar halo
- Globular clusters
  - metallicity and age distributions
- Galactic satellites
  - spatial and metallicity distributions

Old stellar components in the Milky Way

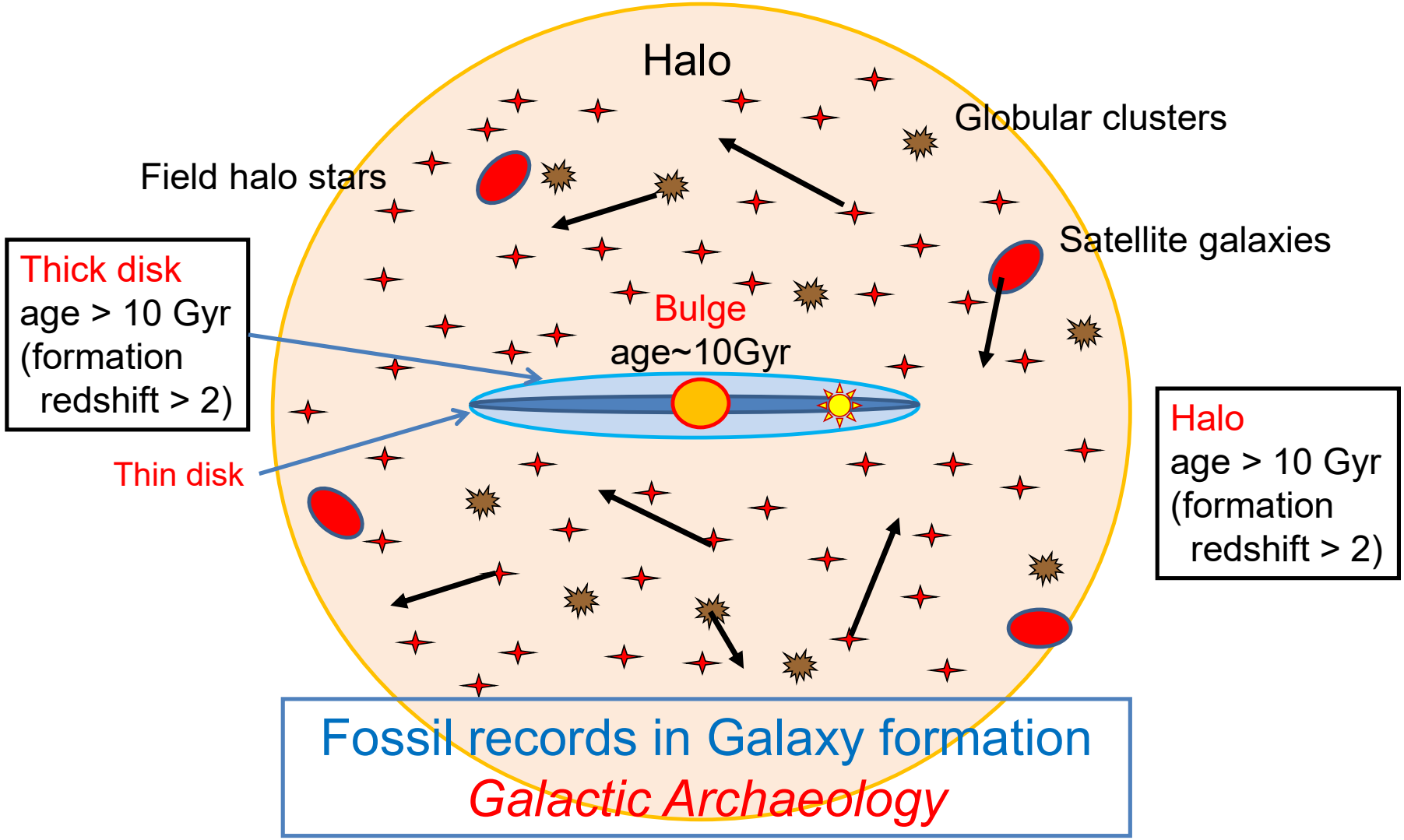

Lookback formation time of stellar components

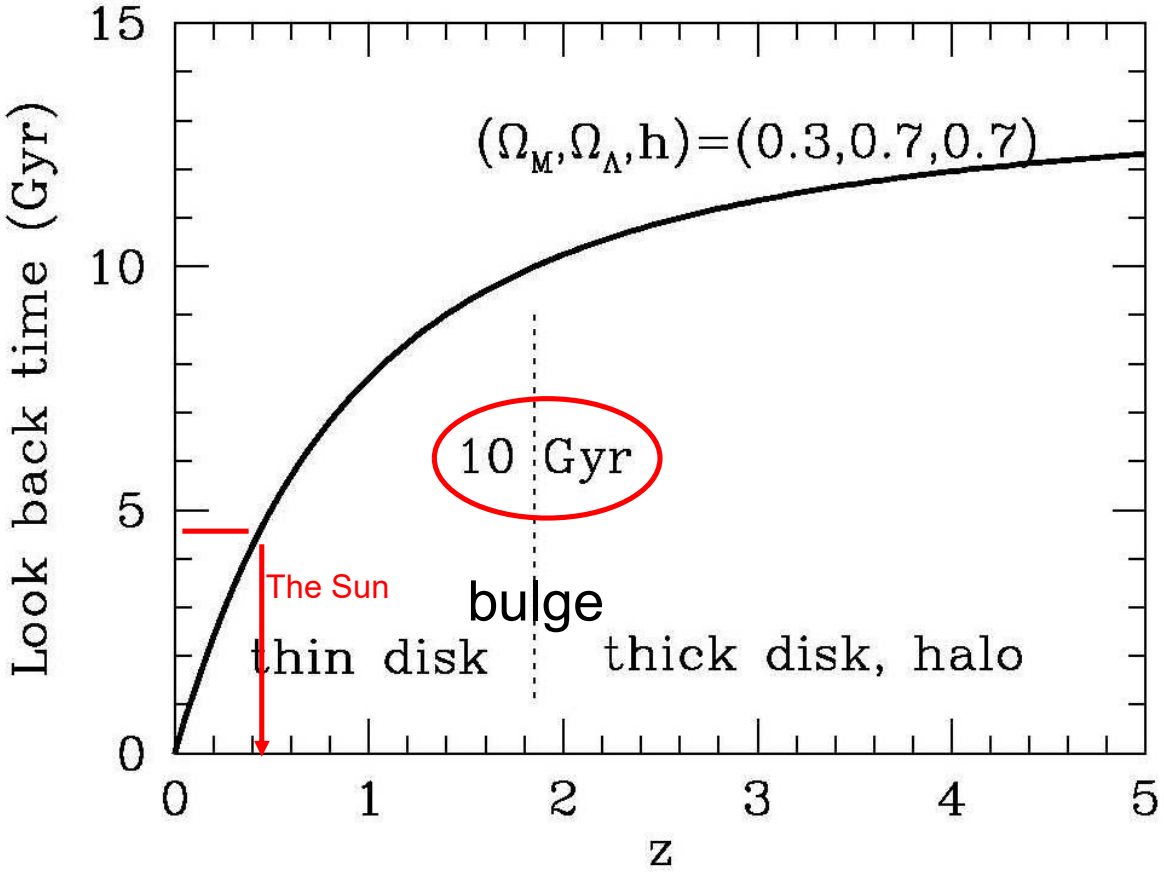

Fossil records of galaxy formation
⇒ Near-field cosmology

3.1 Galactic bulge

Large ISM extinction
⇒IR Obs

Bulge stars in the NIR CM-diagram
(using photometric data)

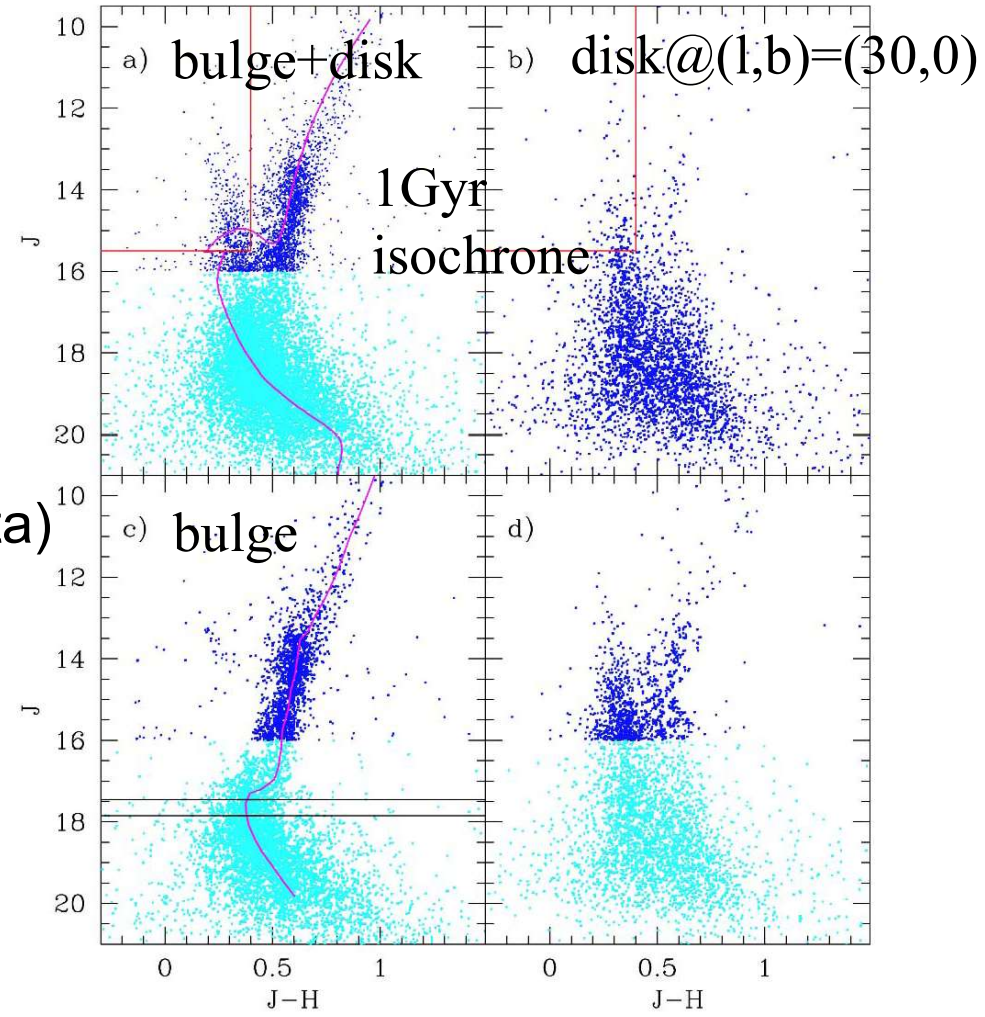

Zoccali et al. 2003,
A&A, 399, 931

Fig. 5. a) The CMD of the bulge field. The solid line is the 1 Gyr isochrone for a solar metallicity population. **b)** CMD of the disk control field in the direction $(l, b) = (30, 0)$. The region inside the box has been used to normalize the number of disk stars seen through the bulge line of sight. **c)** CMD of the bulge field as statistically decontaminated from the disk population. The horizontal lines locate the main sequence turnoff at $J = 17.65 \pm 0.2$. The ridge line of the CMD is also shown. **d)** Stars that were subtracted from the bulge CMD in order to obtain the decontaminated CMD.

Zoccali et al. 2003

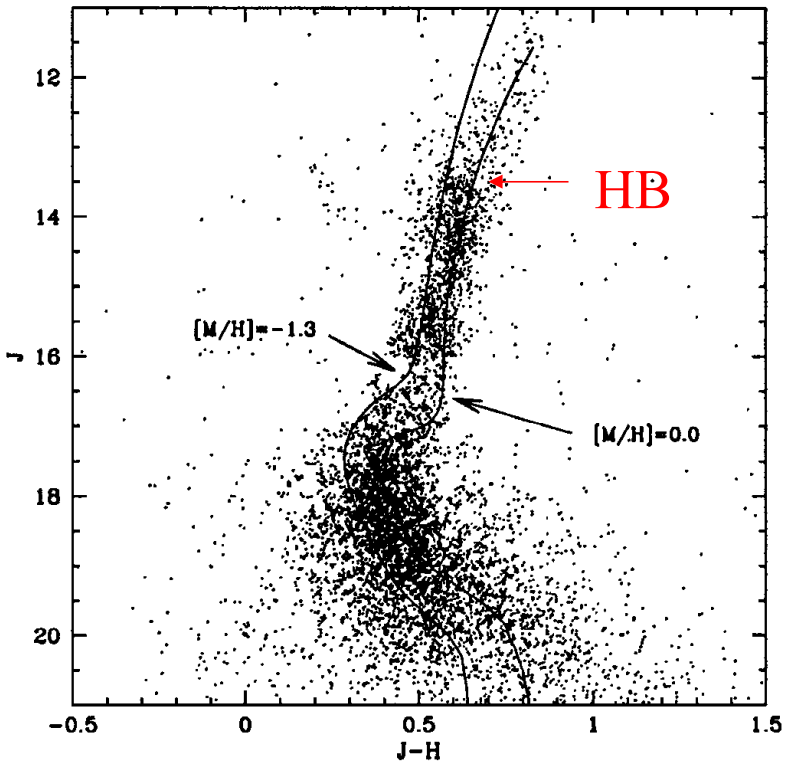

Fig. 24. 10 Gyr isochrones (Cassisi & Salaris 1997) for the two extremes of the bulge MD are overplotted on the CMD.

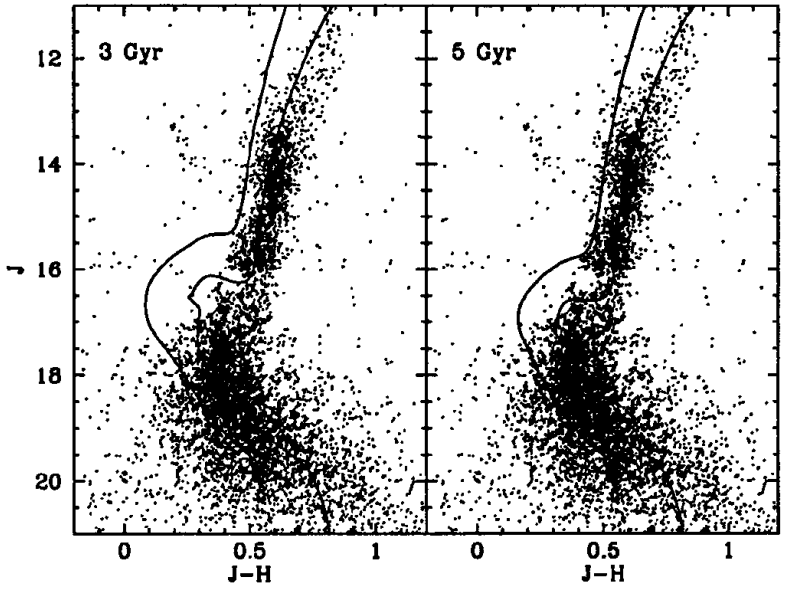

Fig. 25. Comparison of the bulge CMD with two younger isochrones of 3 (left panel) and 5 Gyr (right panel). Two models are plotted in each panel, both referring to the same age. The reddest curve in each panel is for solar metallicity, while the one on the blue side is for [M/H] = −1.3.

10Gyr isochrone
at overall metallicity [M/H]=-1.3, 0.0

3 & 5 Gyr isochrone
at [M/H]=-1.3, 0.0

Distributions of [Fe/H] and [Mg/Fe] in Galactic Bulge

Bensby et al. 2013

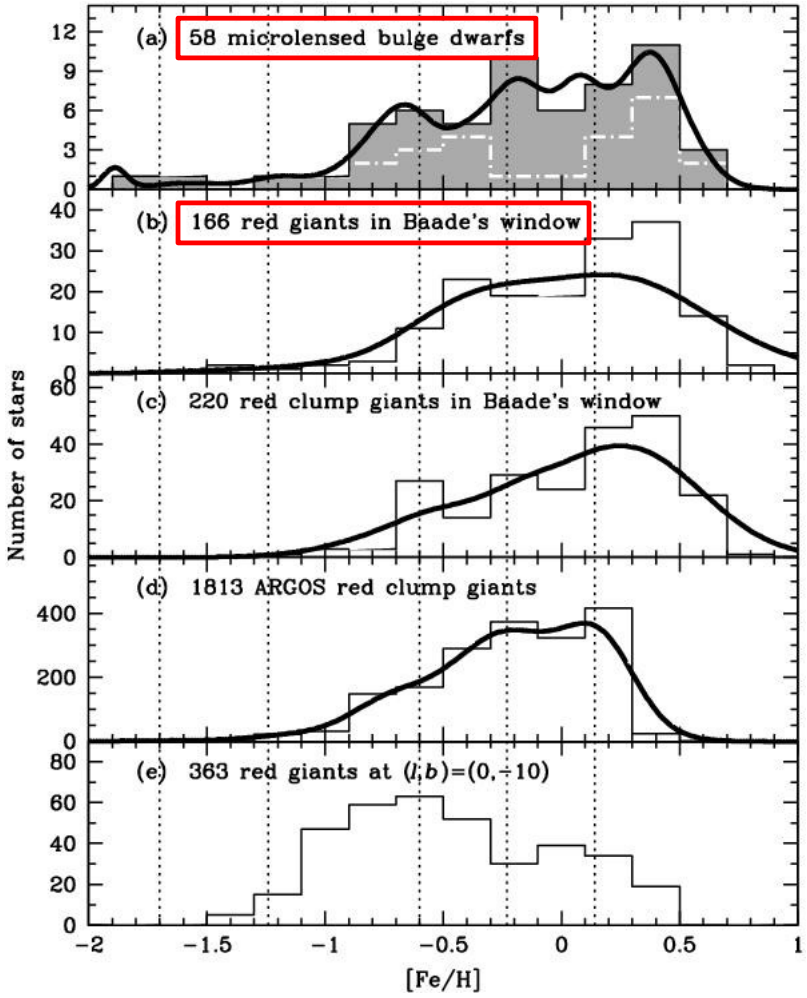

Alves-Brito et al. 2010
(for RGBs)

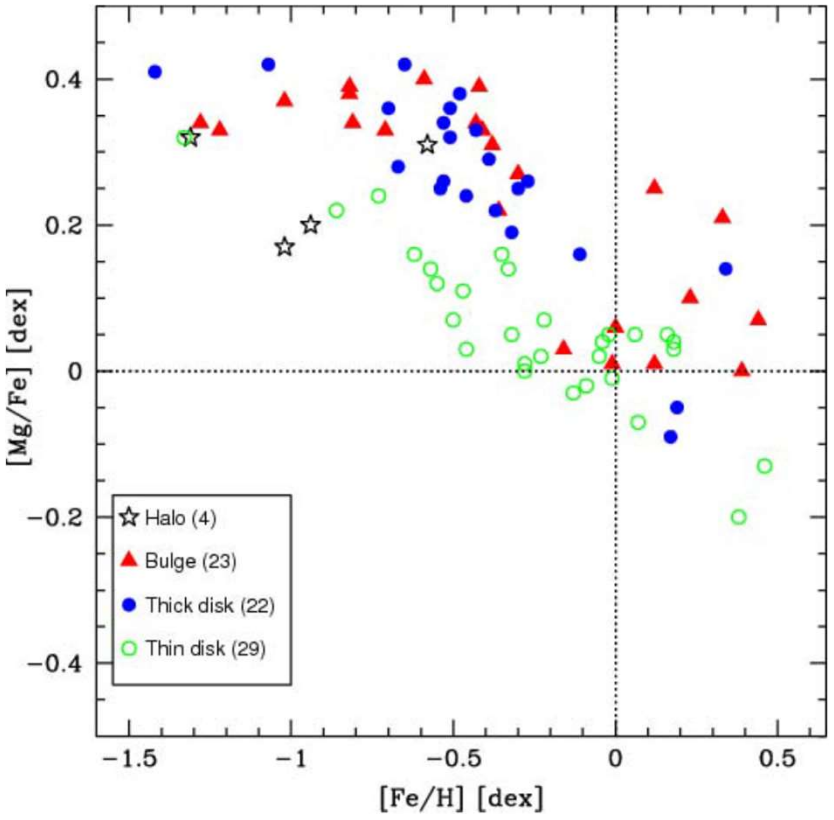

Abundance of α-elements for bulge/disk dwarfs

(Bensby et al. 2013)

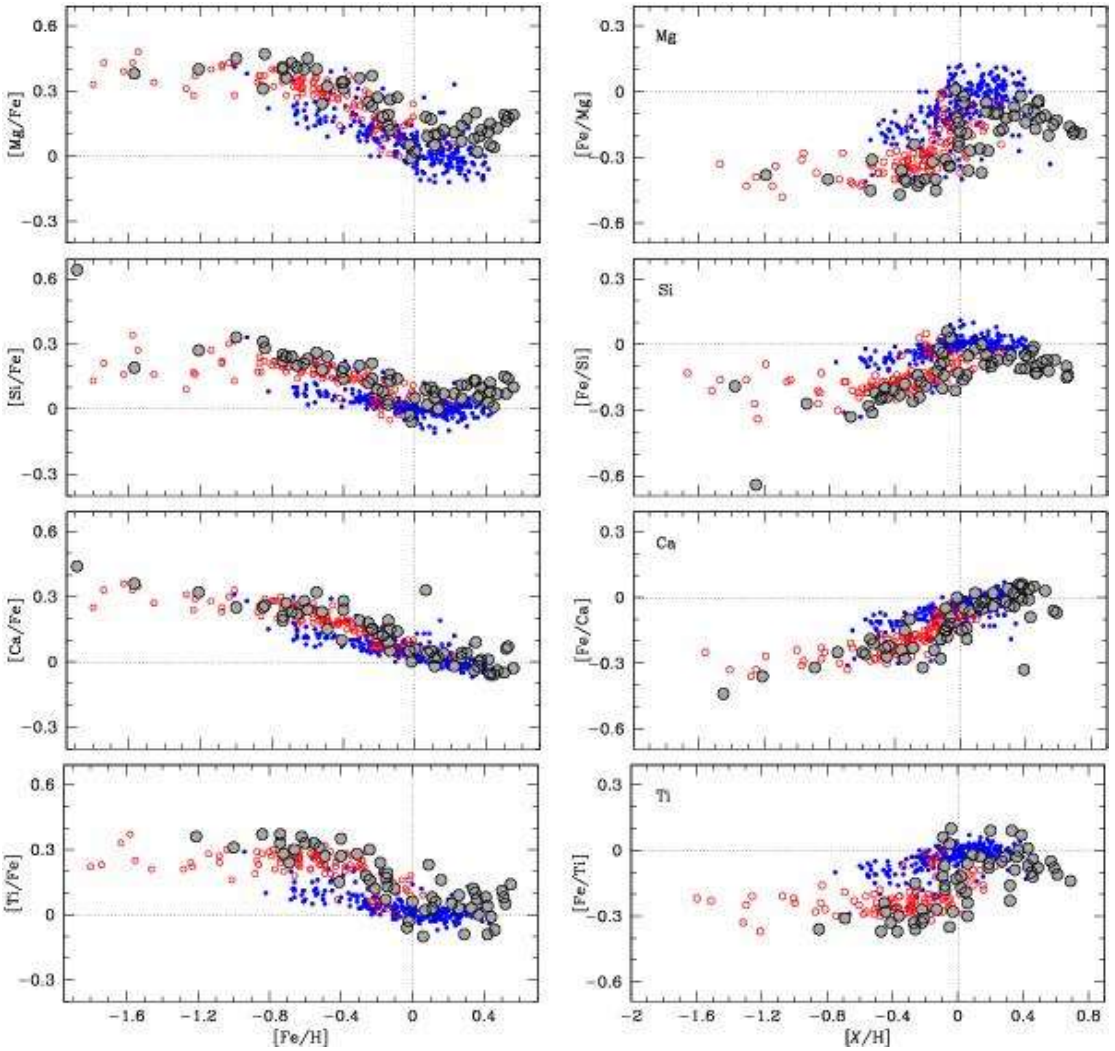

Filled grey: bulge
Red: thick disk
Blue: thin disk

Bulge stars show highest [α/Fe] at given [Fe/H]

Age distribution for bulge dwarfs

(Bensby et al. 2013)

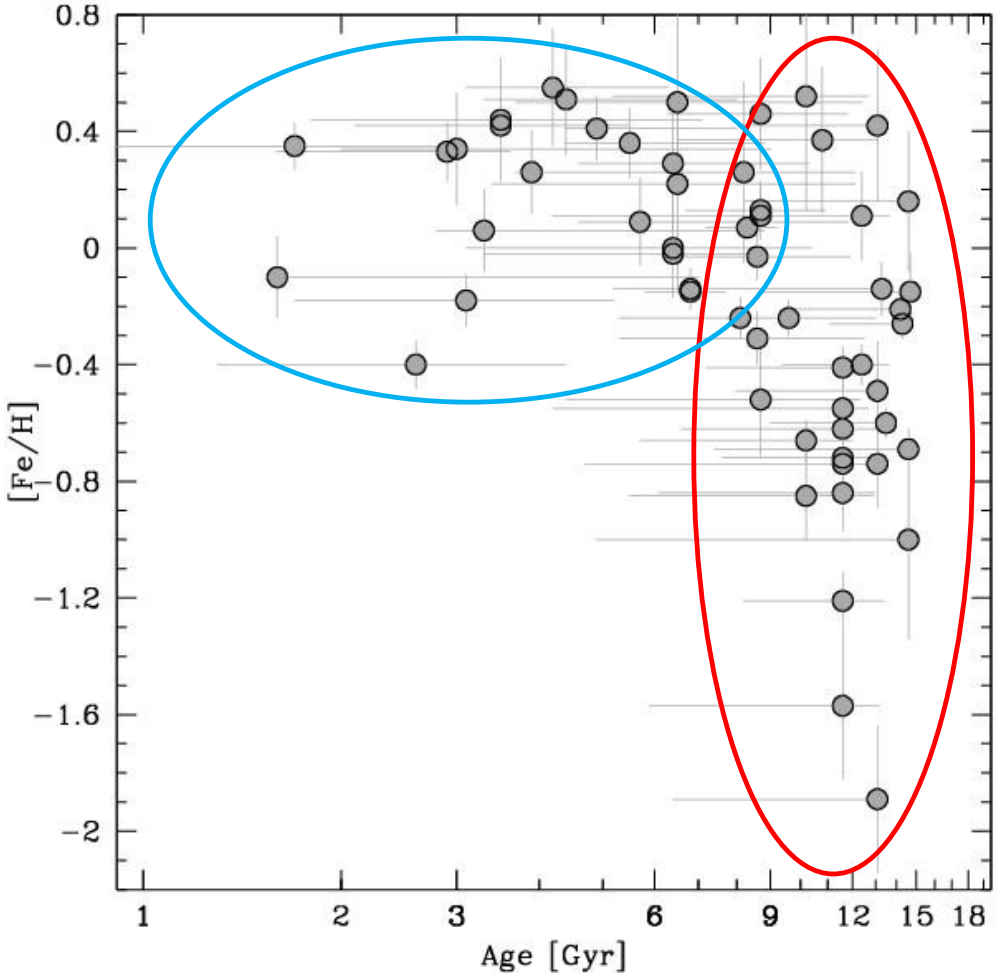

BRAVA (Bulge Radial Velocity Assay)
Howard+ 2009

COBE image

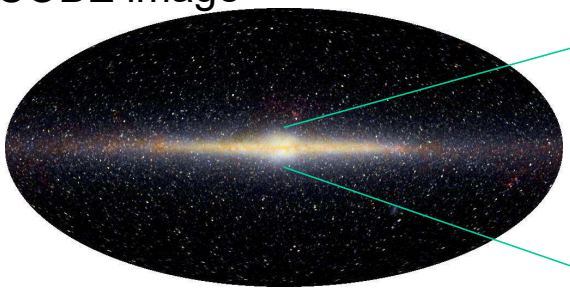

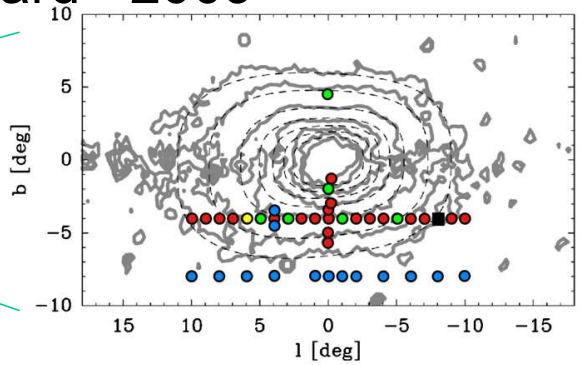

COBE 2μm image

BRAVA survey fields

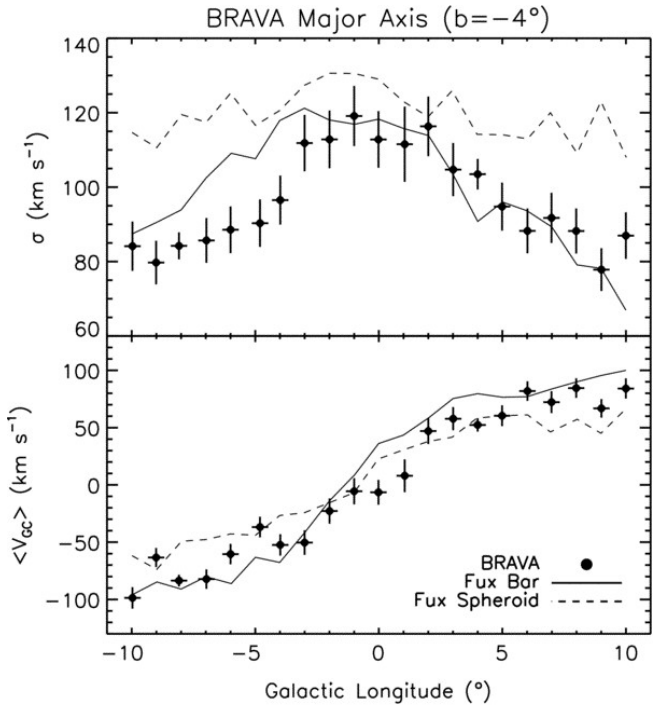

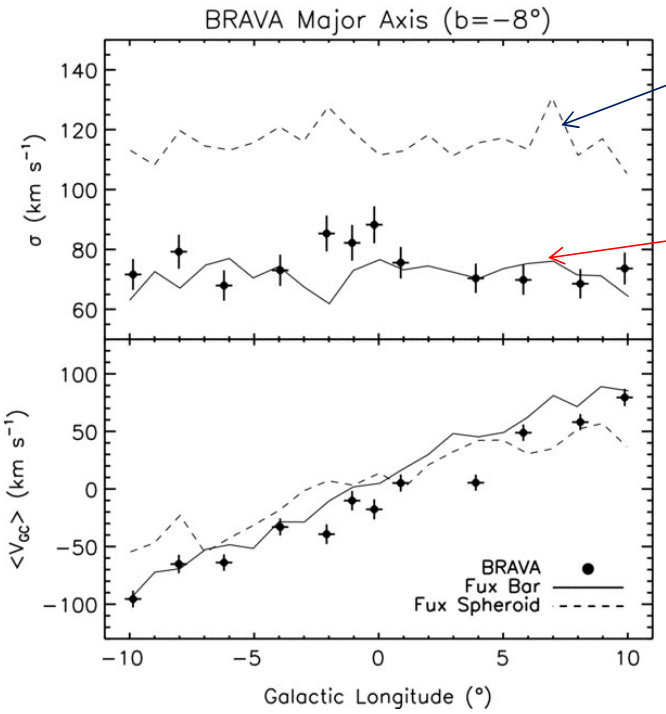

Spheroid

Bar

* Cylindrical rotation
* No classical bulge with hot dynamics

3D structure of a boxy/peanut shape bar

Athanassoula (2005)

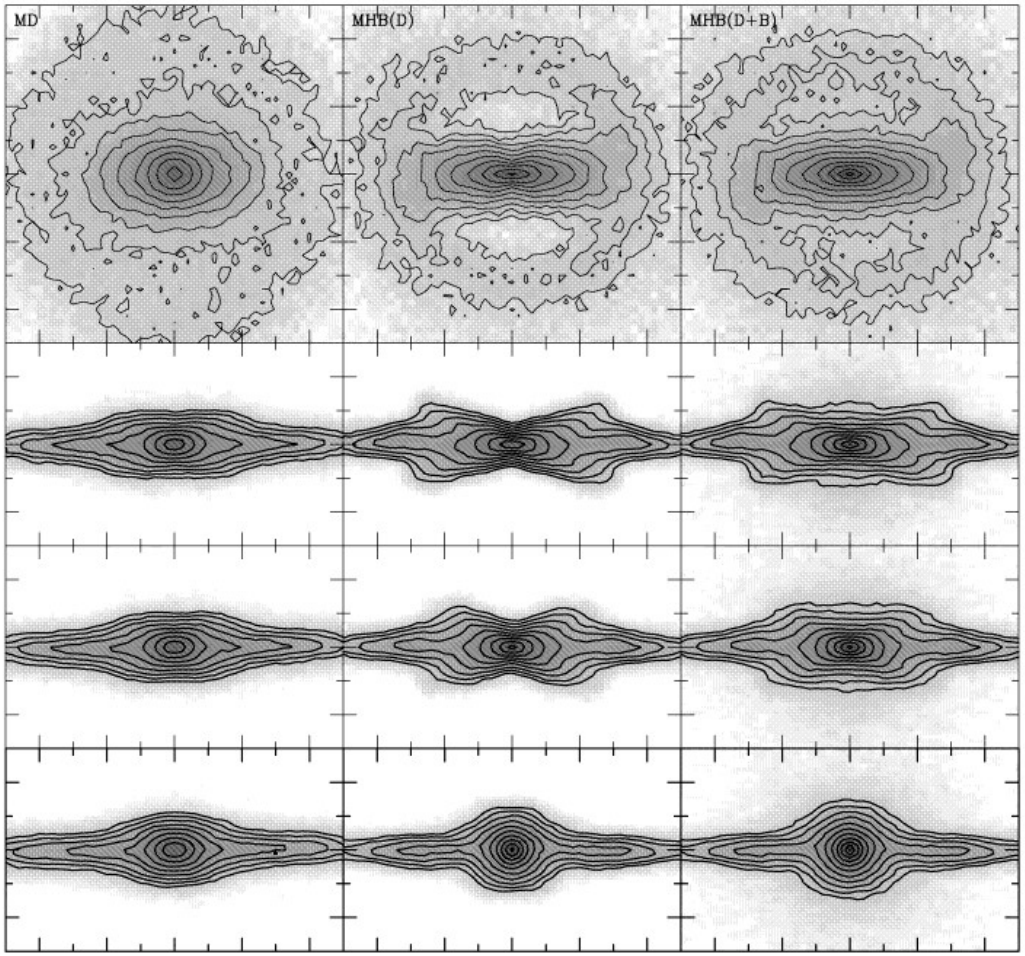

Figure 1. Face-on (top row), side-on (second row), 45° viewing angle (third row) and end-on (bottom row) views for two characteristic simulations. The projected density is given by grey-scale and also by isocontours (spaced logarithmically). The left-hand column of panels illustrates a simulation of MD type, while the central and right-hand columns show a simulation of MHB type. In the central panels only the disc component is shown, while in the right-hand ones both the material from the disc and the classical bulge are shown. The distance between two large tick marks is 2 initial disc scalelengths. The type of the simulation is given in the upper left-hand corner of the upper panels.

Orbits in a bar

Edge-on

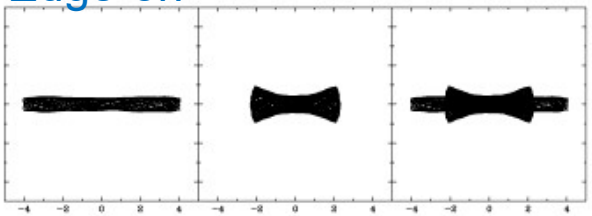

Face-on

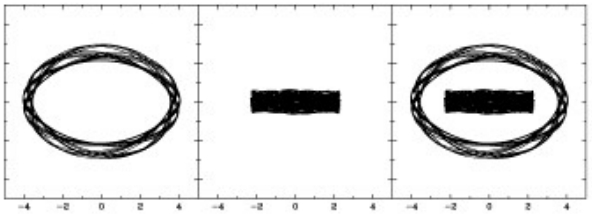

Figure 7. Face-on (lower panels) and side-on (upper panels) views of two orbits in a barred potential, originating from a simulation with a strong bar and peanut. Both orbits are trapped around periodic orbits which are members of the x_1 tree. The right-hand panels show the superposition of the two orbits.

Galactic Bulge: summary

- Old age: ~ 10 Gyr
- Broad metallicity distribution function (MDF)
  - -1 < [Fe/H] < 0, metal-rich stars are dominant.
- Alpha enhanced
  - Enrichment by Type II SNe (time scale < 1 Gyr)
- Boxy/peanut shape with cylindrical rotation
  - Resembling 3d dynamical structure of a bar (pseudobulge) which formed via disk instability from old disk stars
  - No or small fraction of a classical bulge or spheroid, which is formed via major merger?

Bulge formation by disk instability?

3.2 Galactic disk

Star counts toward the Galactic pole:
discovery of the thick disk component

Gilmore & Reid (1983)

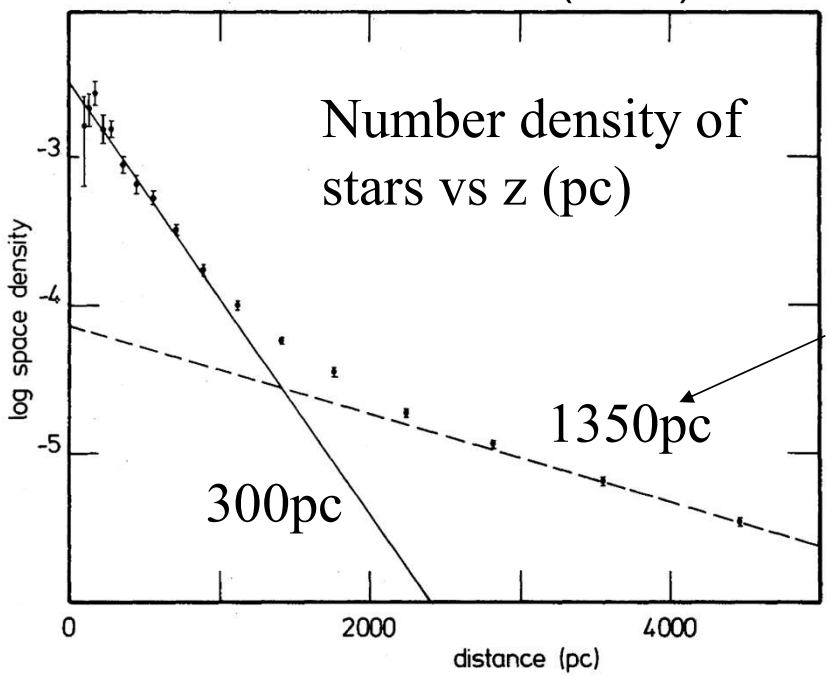

Exponential scale height h_z

	h_z(kpc)	σ_R(km/s)	σ_z(km/s)	<Vφ>(km/s)
Thin disk	~0.3	34	18	220
Thick disk	~1.0	61	39	200

Edvardsson et al. 1993

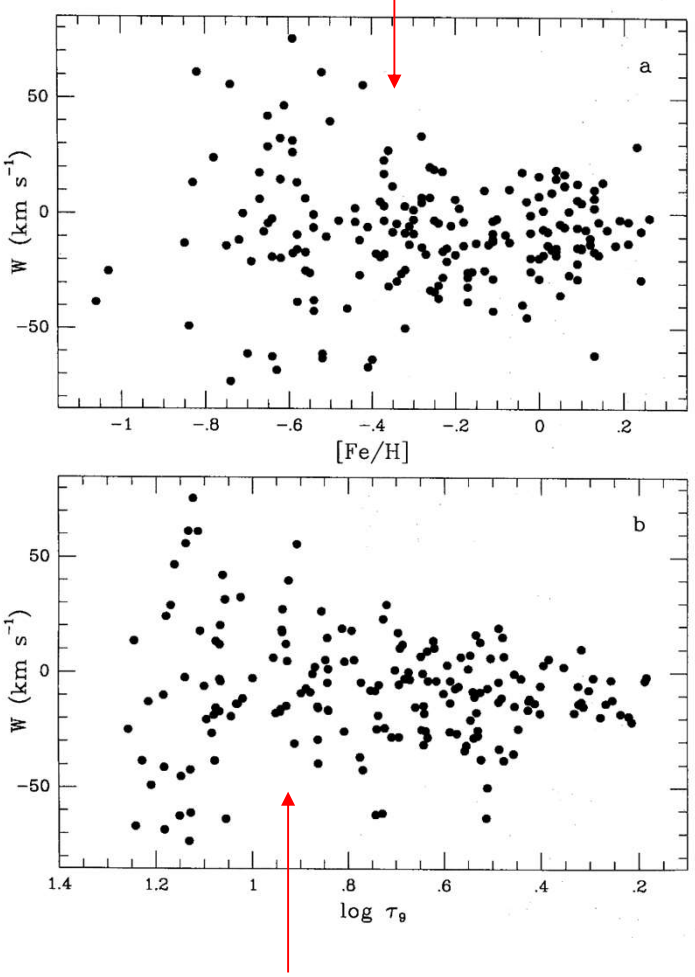

Thick disk stars
at [Fe/H] < -0.4, age >10Gyr

Quillen & Garnett, astro-ph/0004210

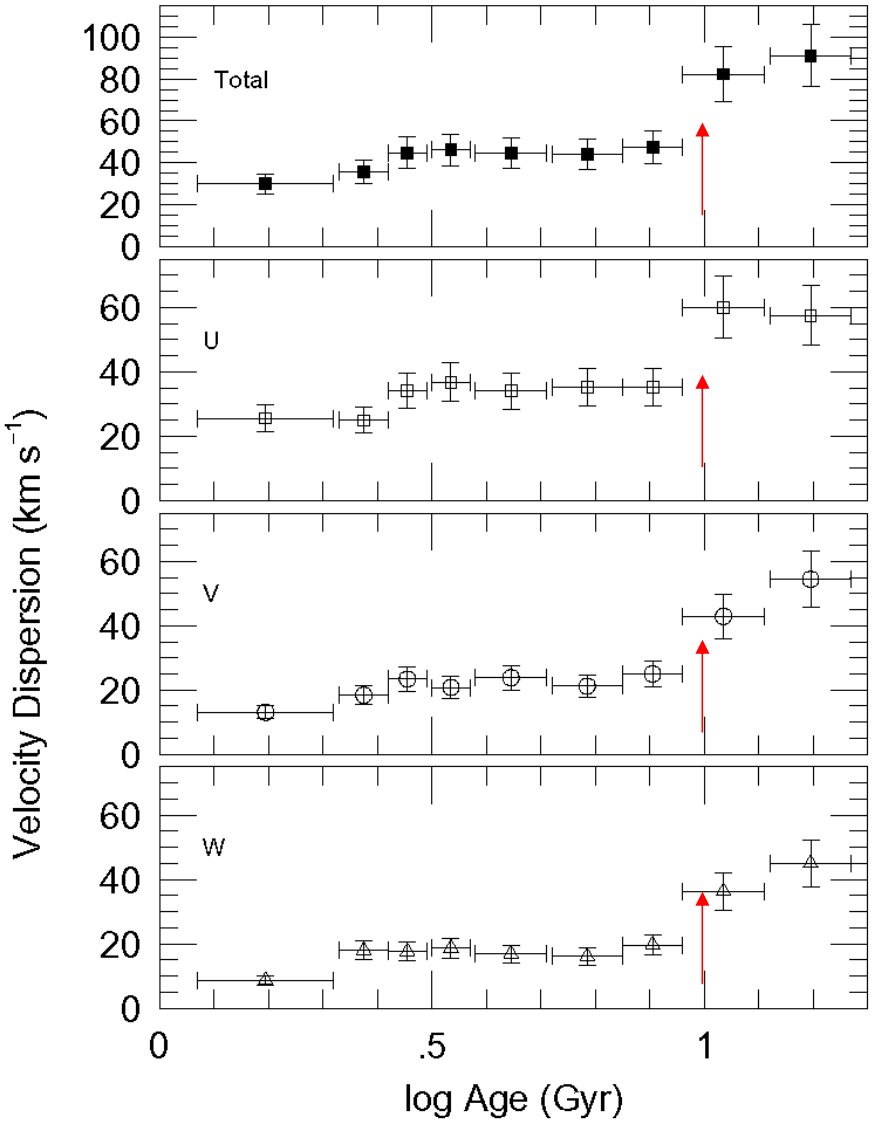

Feltzing et al. 2003
High [α/Fe] thick-disk stars

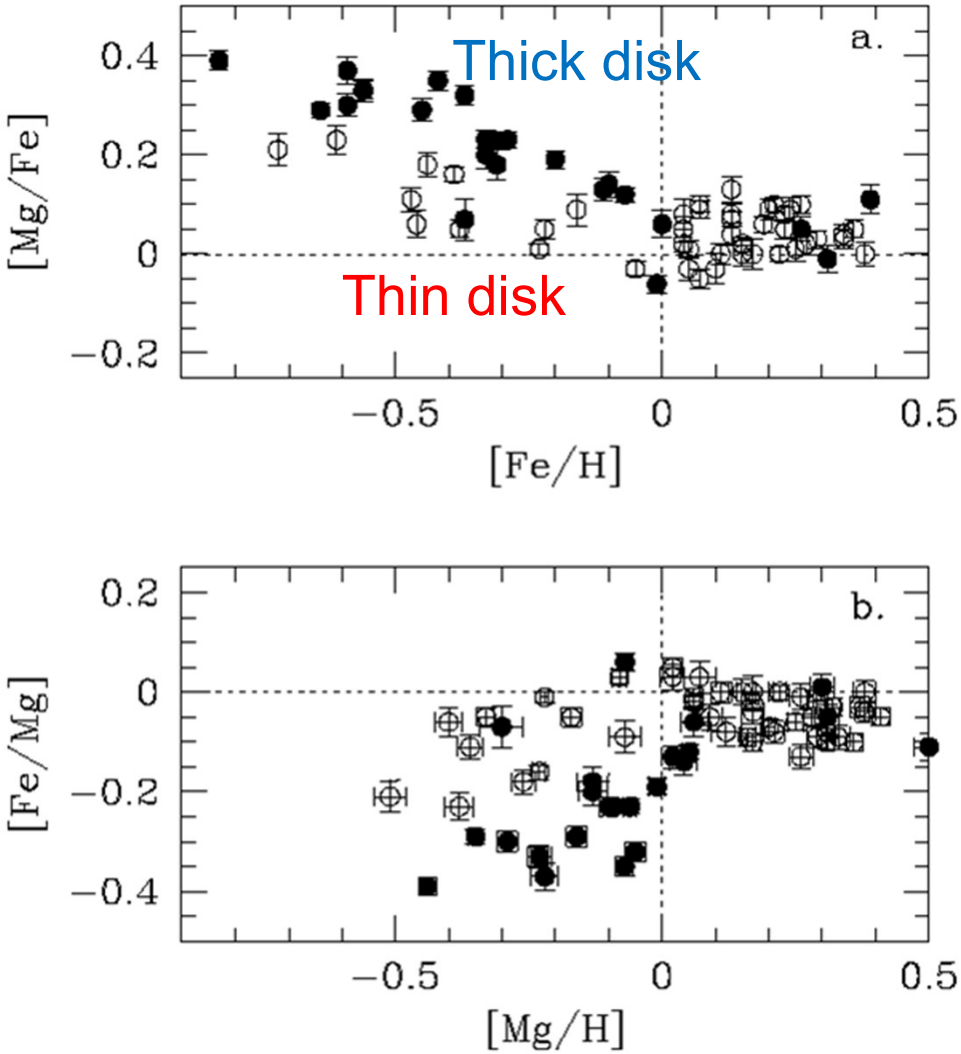

Van der Kruit & Searle 1981
Thick disk in NGC4565

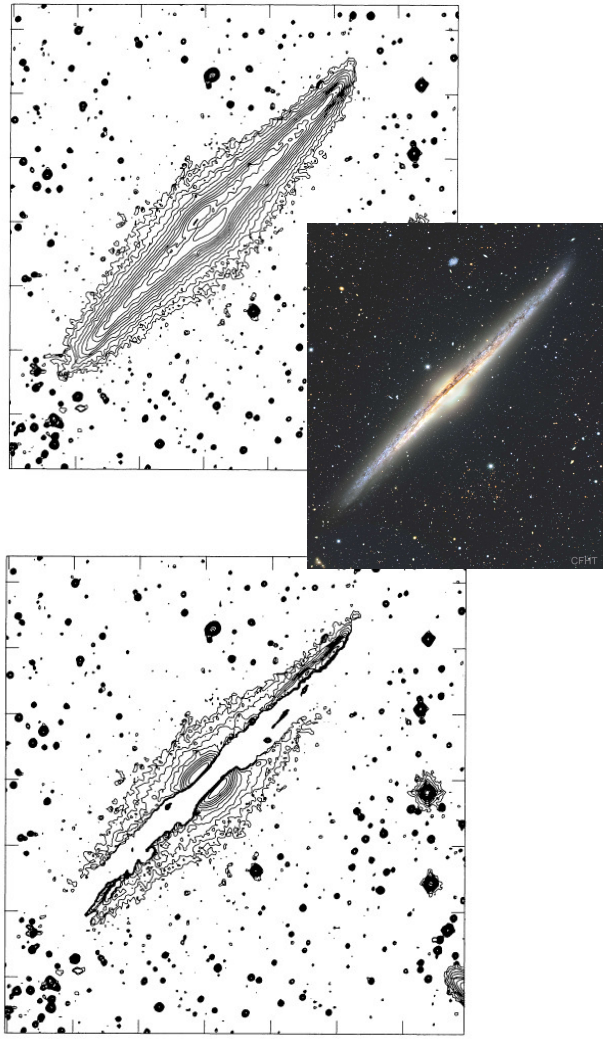

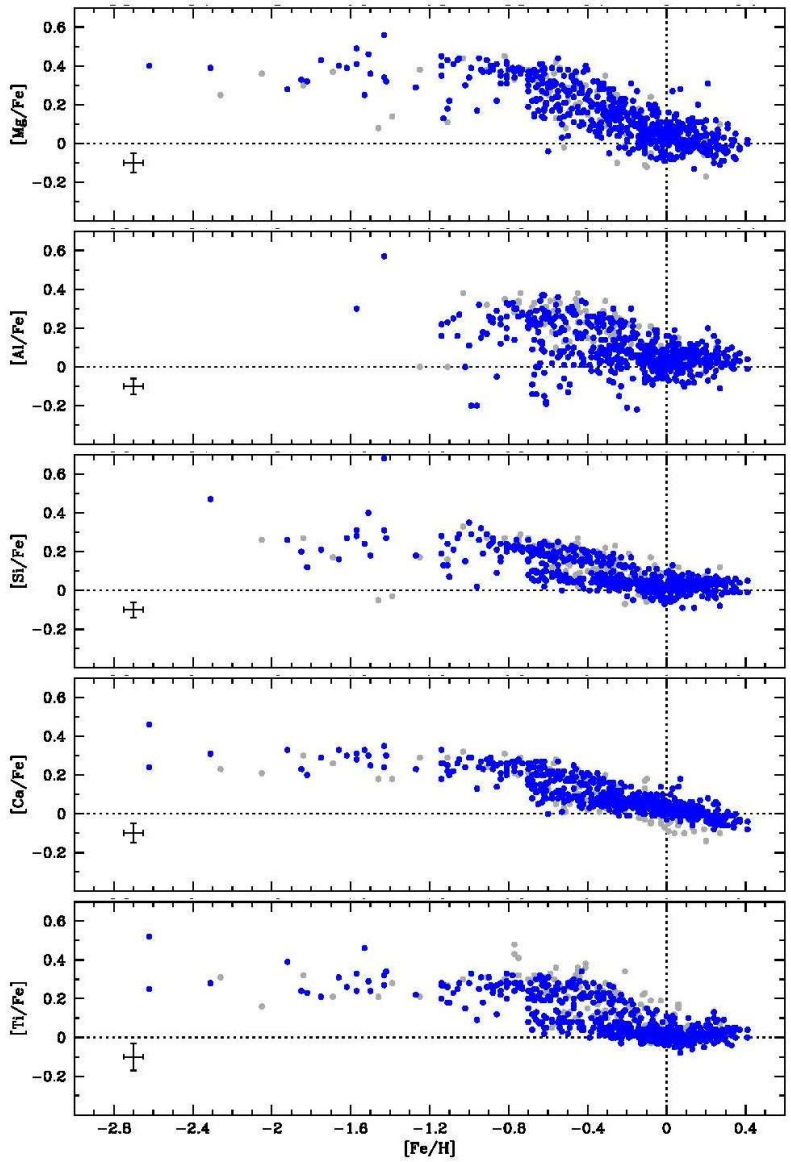

[alpha-elements/Fe]
= Type II SNe / Type Ia SNe

Chemical clock diagram

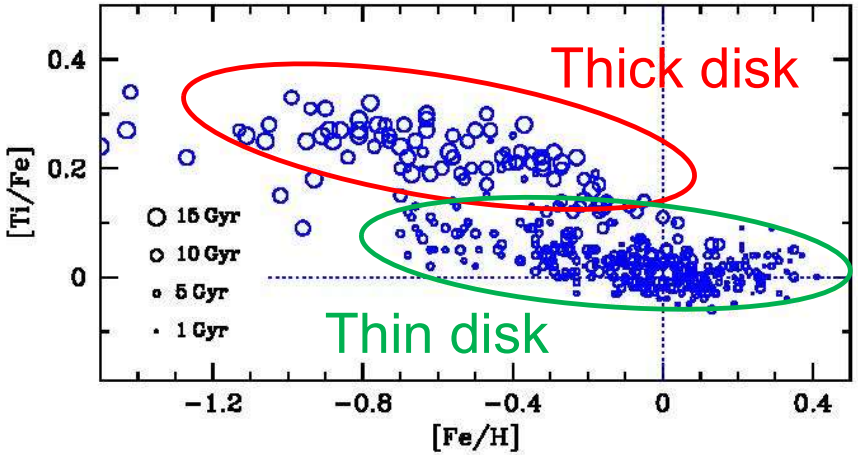

Bensby+ 2014

[α/Fe] vs. [Fe/H] at different R - SDSS/APOGEE

Anders+2014

Presence of separate high [α/Fe] + low scale-length component

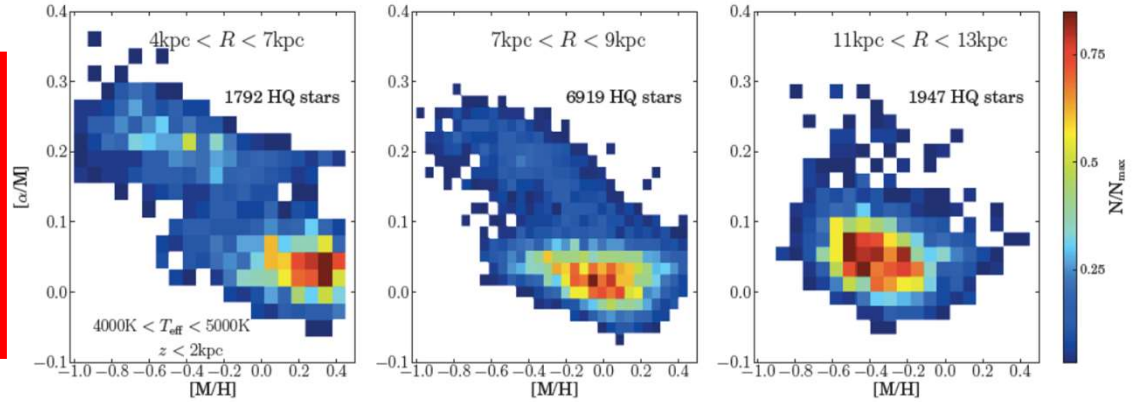

Hayden+15

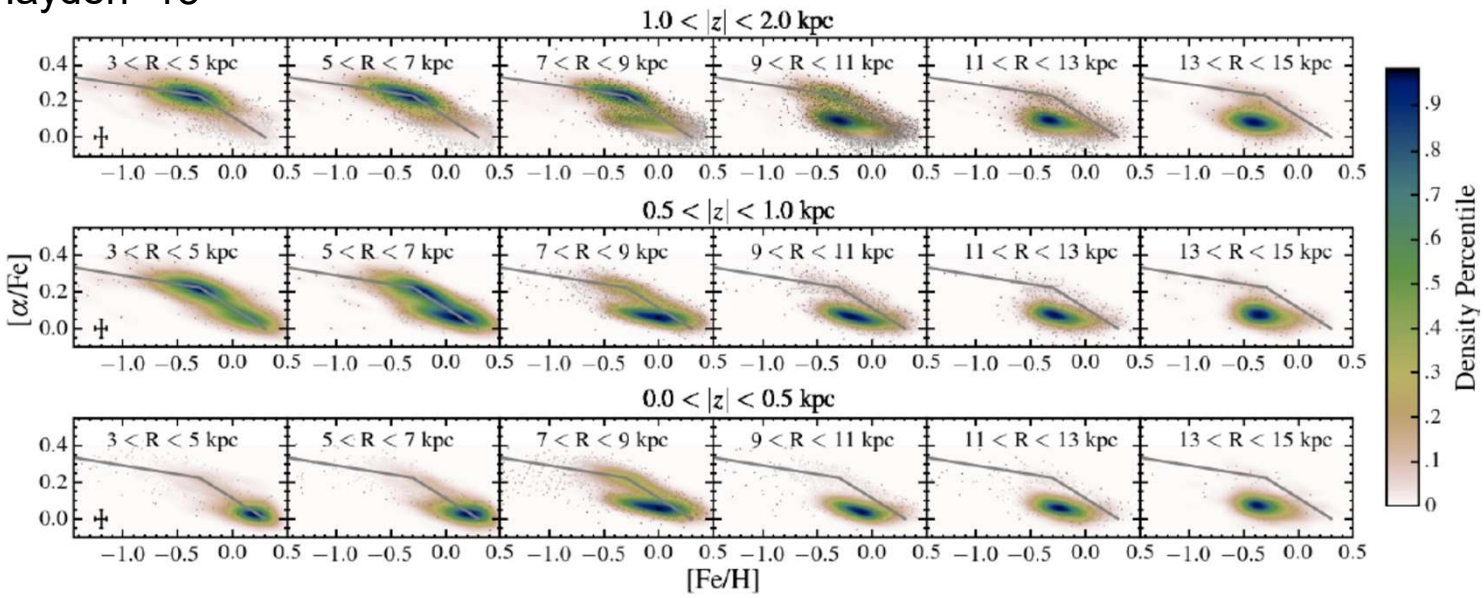

Age-Metallicity Relation (AMR)

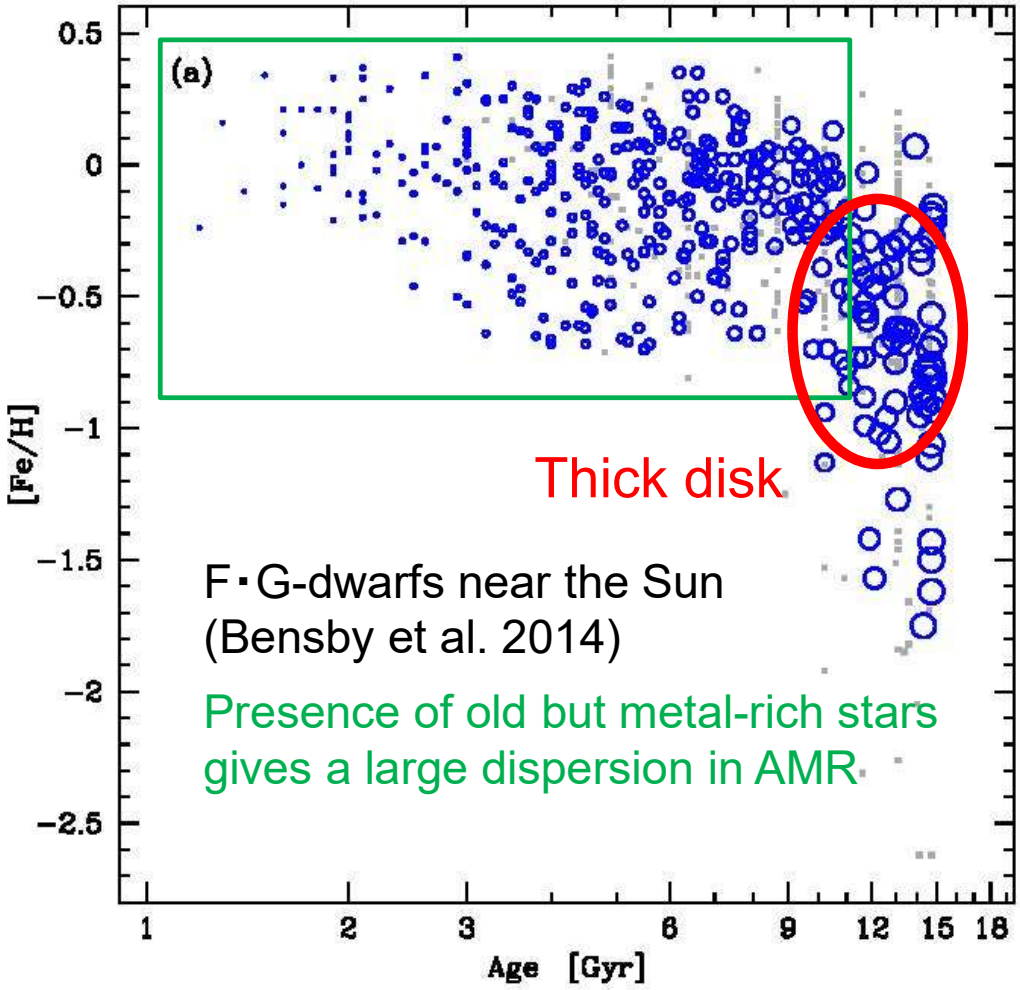

Xiang & Rix 2022

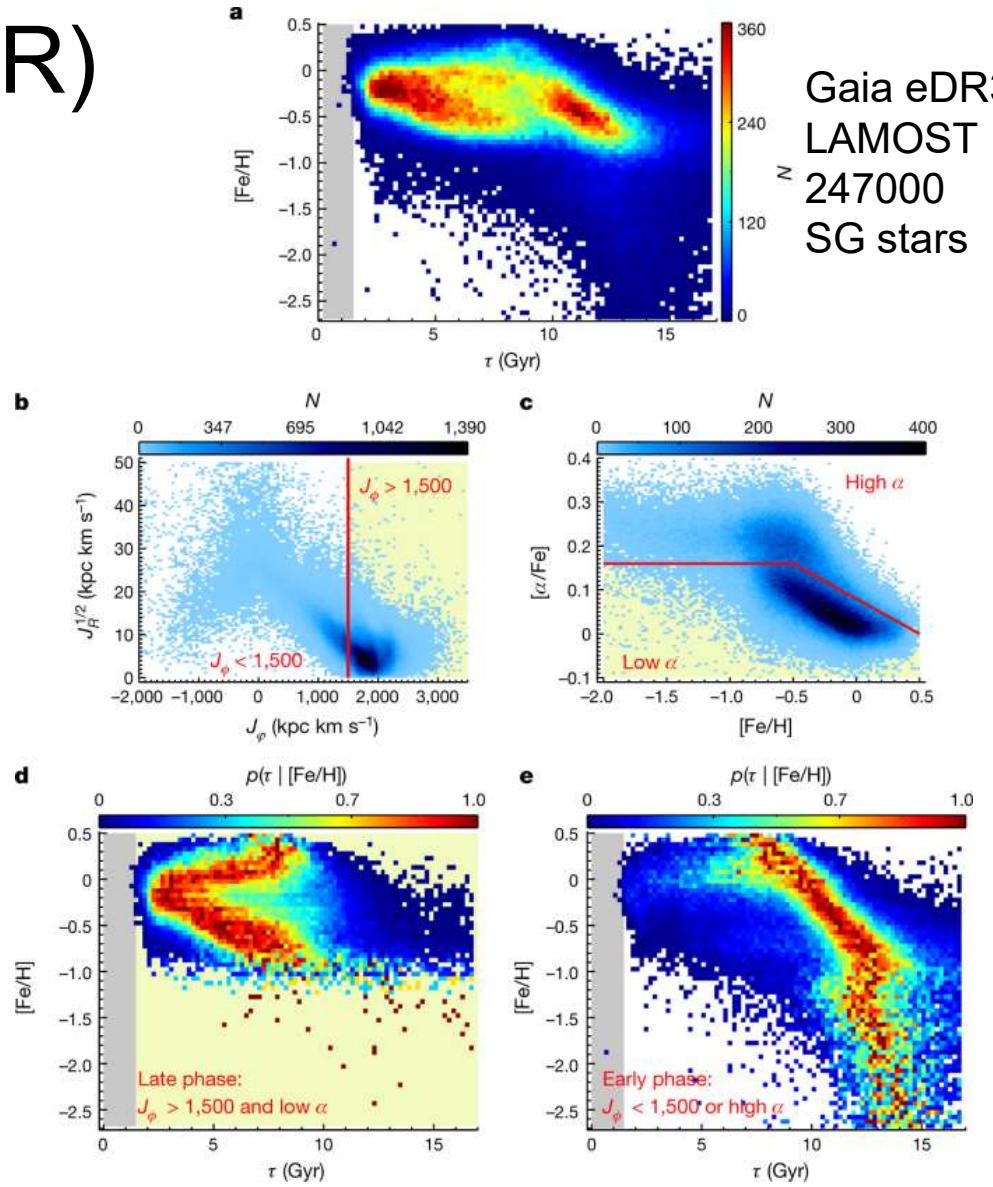

Gaia eDR3
LAMOST
247000
SG stars

Metallicity distribution of the thick disk

(reproduced from Wyse & Gilmore 1995)

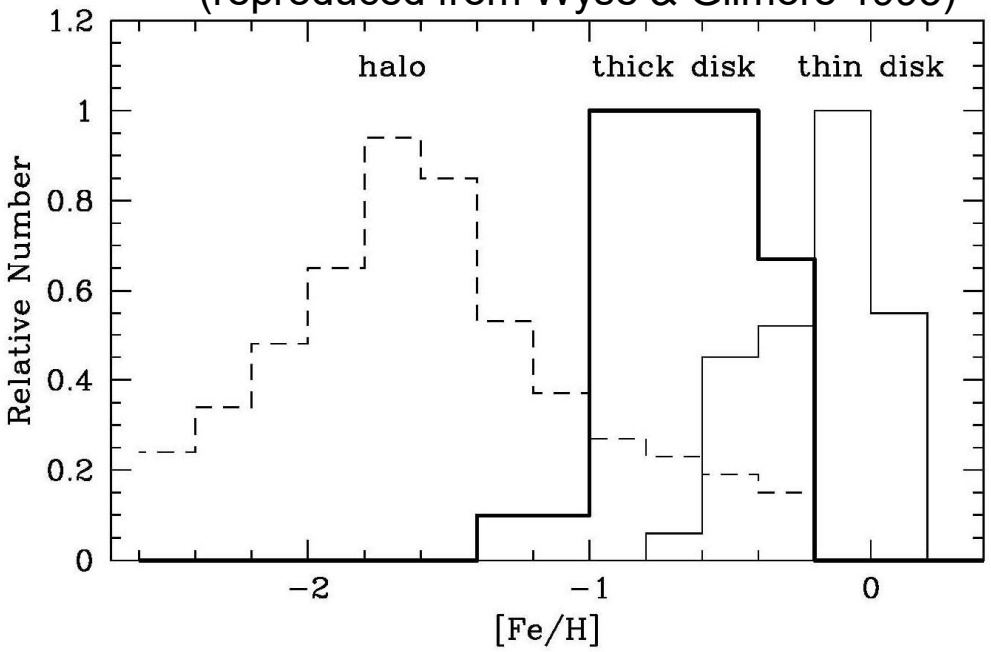

(Chiba & Beers 2000)

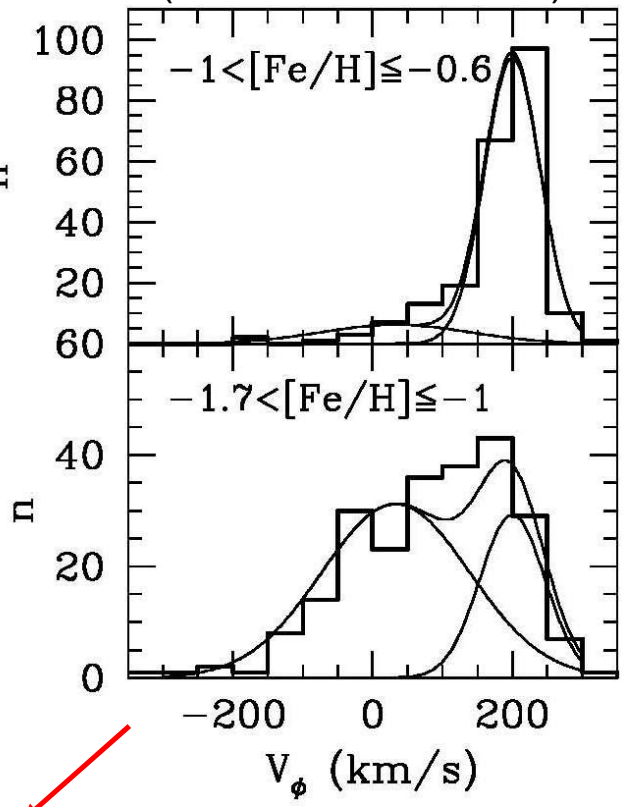

fiducial metallicity range of the thick disk
-1 < [Fe/H] < -0.4

But the rapidly-rotating disk component is extended toward lower metallicity: Metal-Weak Thick Disk (MWTD)

Thin disk vs. Thick disk

<V_ϕ> (km/s)

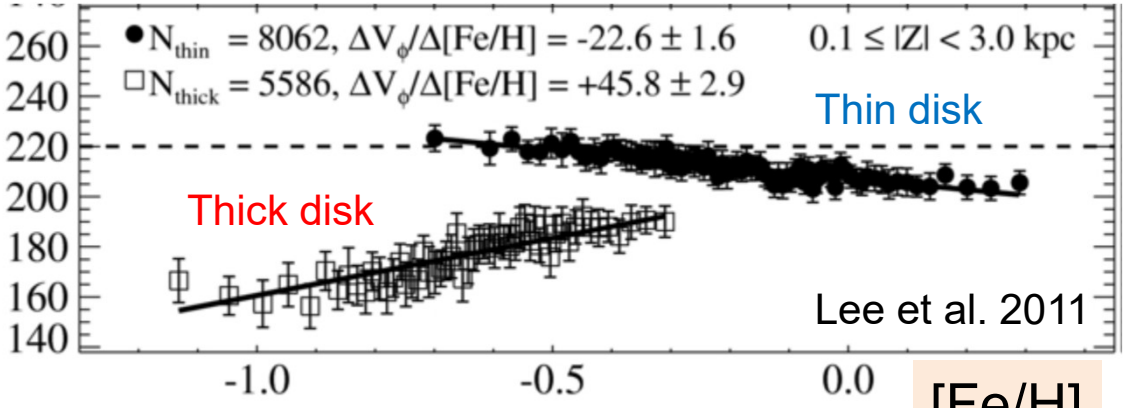

Positive gradient

Negative gradient

[Fe/H]

[Fe/H]

SDSS sample

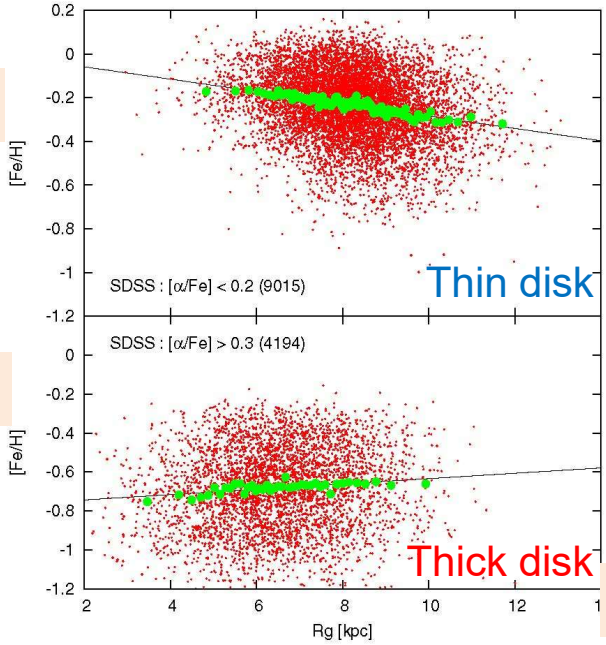

Toyouchi & Chiba 2014

[Fe/H]

Thin disk
Negative gradient

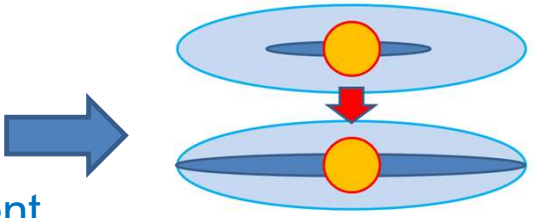

Inside-out formation

Thick disk
Positive gradient

?

Mean orbital radius(kpc)

Evidence that the Galactic disk has been disturbed

Gaia DR2
Phase-space distribution
for nearby stars

Evidence for
recent disturbance events
(e.g. by satellite infall)
and relaxation via
Phase mixing

Antoja et al. 2018, Nature

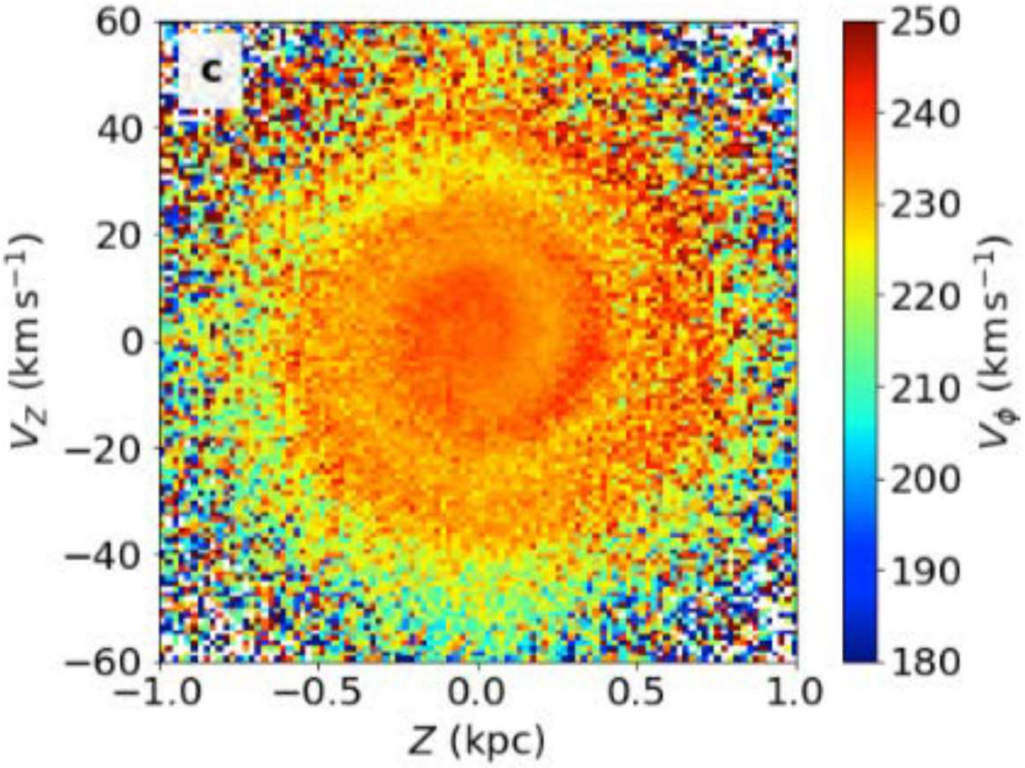

3.3 Galactic halo

Ryan & Norris 1991, AJ, 101, 1865 (before Gaia)

High velocity stars observed from the Sun

(V < -220 km/s) ⇒ 372 stars belonging to the halo

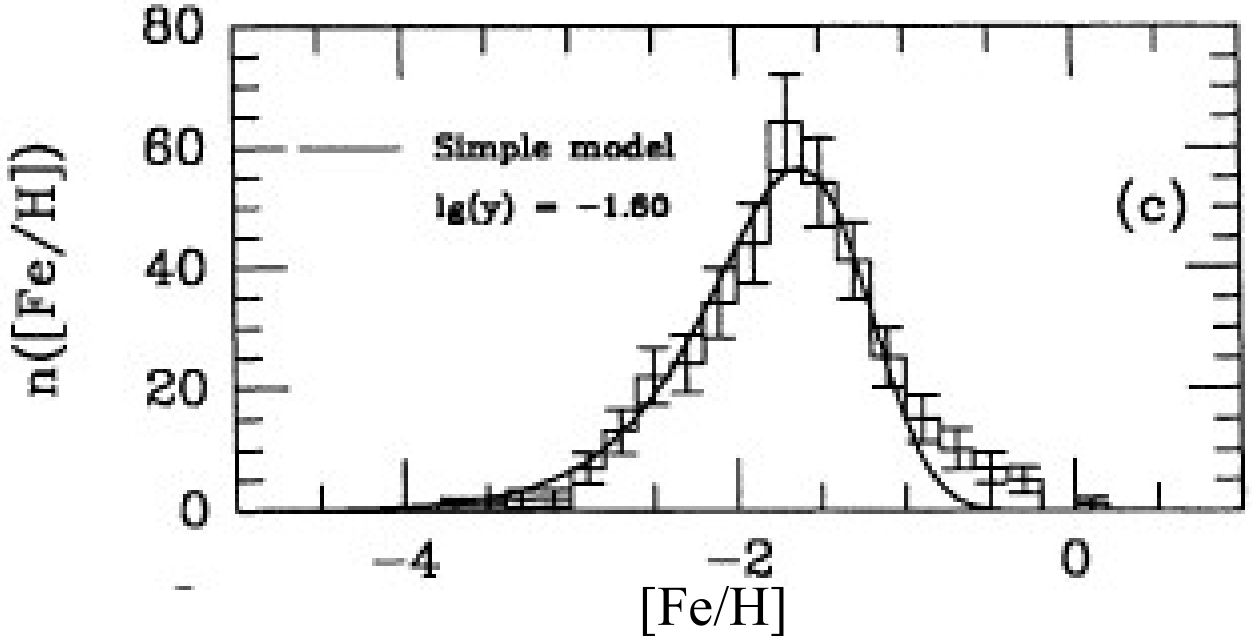

Typical metallicity range of halo stars: [Fe/H] < -1

(A strict selection to avoid disk stars is like [Fe/H] < -1.5)

Recent result using Gaia

Bonaca et al. 2017, ApJ, 845, 101

~ 160,000 stars with Gaia + RAVE/APOGEE (D<3kpc)

⇒ $| V^{tot}_{star} - V_{LSR} |$ > 220 km/s for halo and < 220 km/s for disk

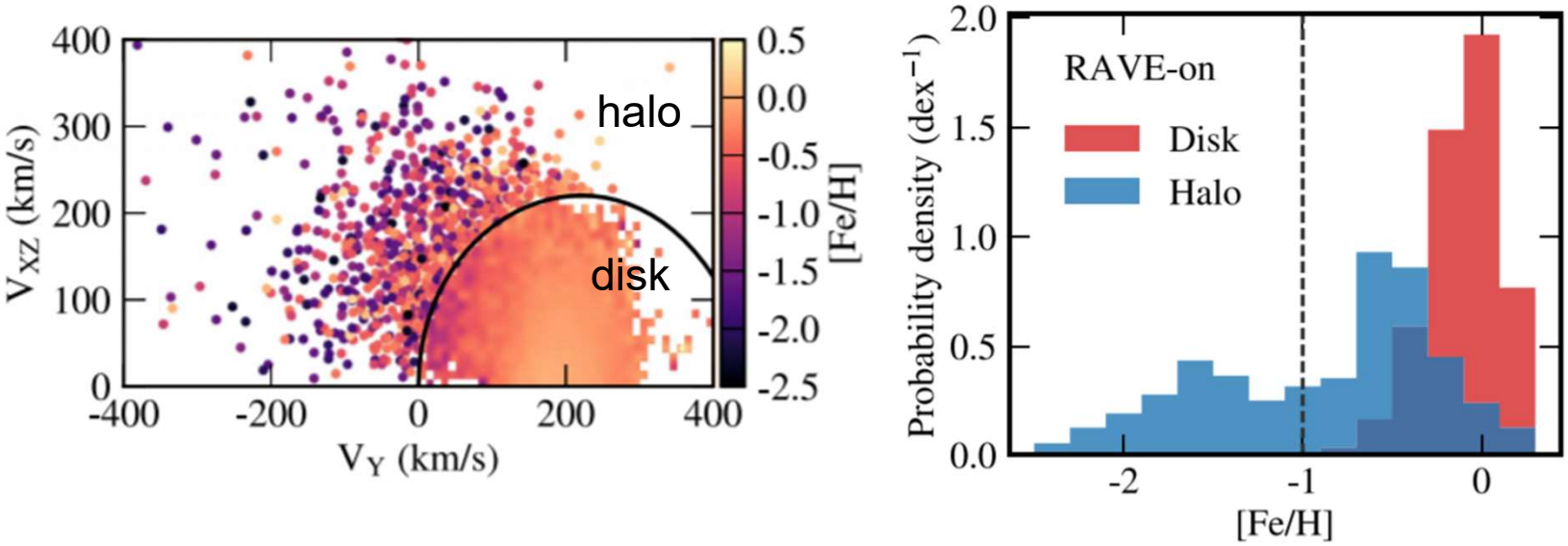

Presence of metal-rich halo stars with [Fe/H] > -1

⇒ what is the origin of these stars ?

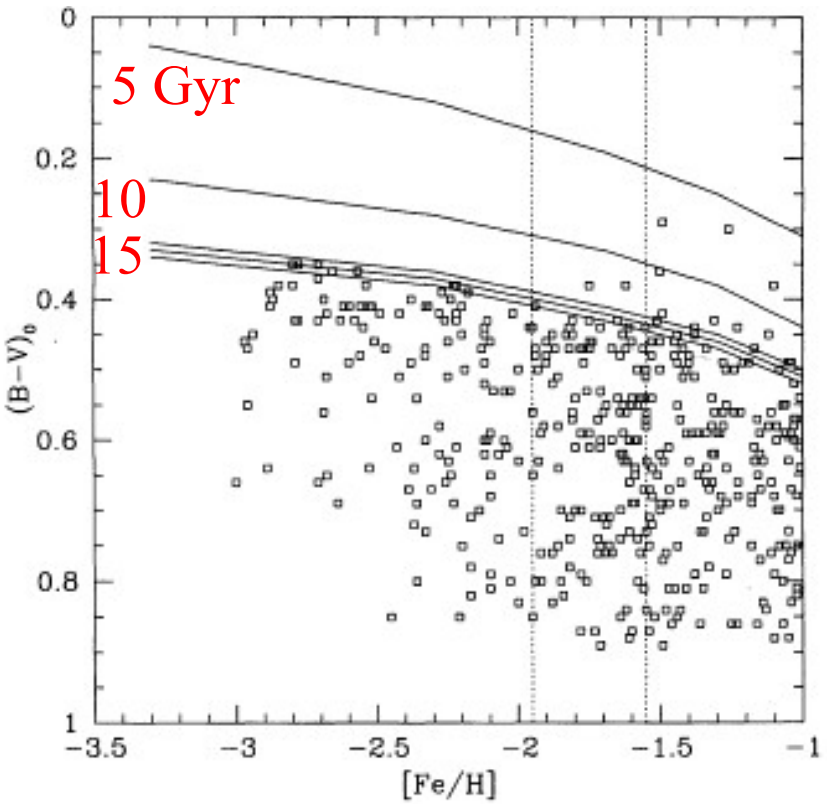

Figure 2. The distribution of dereddened $B-V$ colour and [Fe/H] for metal-poor stars from the proper-motion-selected sample of Carney et al. (1994). Stars with reddening $E(B-V) \geq 0.07$ have been omitted. Uncertainties have been ignored in the interests of clarity, and are of order $\sigma = 0.1$ dex in [Fe/H] and $\sigma = 0.007$ in $B-V$. Superposed are turn-off isochrones (revised Yale Isochrones) with ages of 5, 10, 15, 16 and 17 Gyr (from top to bottom). The vast majority of stars have colours consistent with ages $\gtrsim 15$ Gyr. The three metallicity ranges delineated by the dashed lines are discussed separately.

Unavane, Wyse, Gilmore. (1996)

Halo stars (near the Sun)
are old (>10 Gyr).
Later accreted fraction
< 10%

[α/Fe] for Galactic stars (Venn et al. 2004)

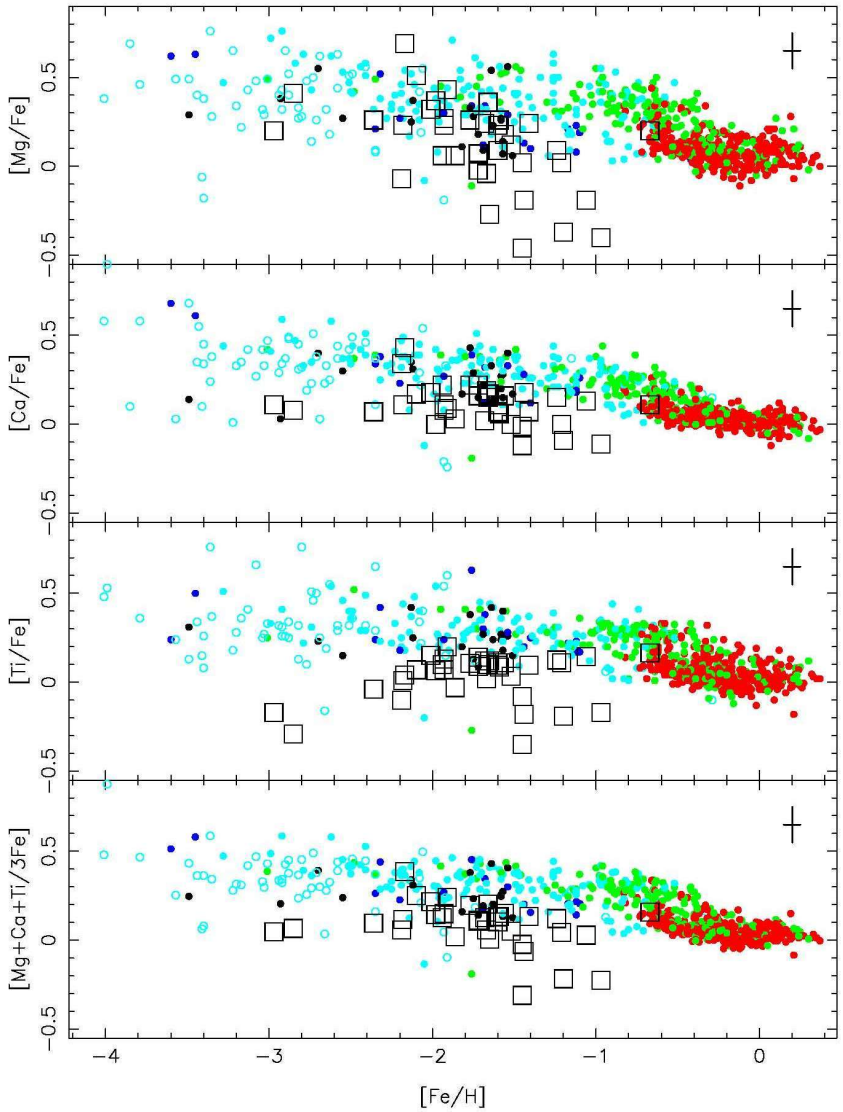

- Halo
- Thick disk
- Thin disk
- Retrograde halo
- Dwarf satellites

Halo and disk stars in abundance-ratio diagram

using Gaia DR2 and APOGEE DR14

Mackereth et al. (2019)

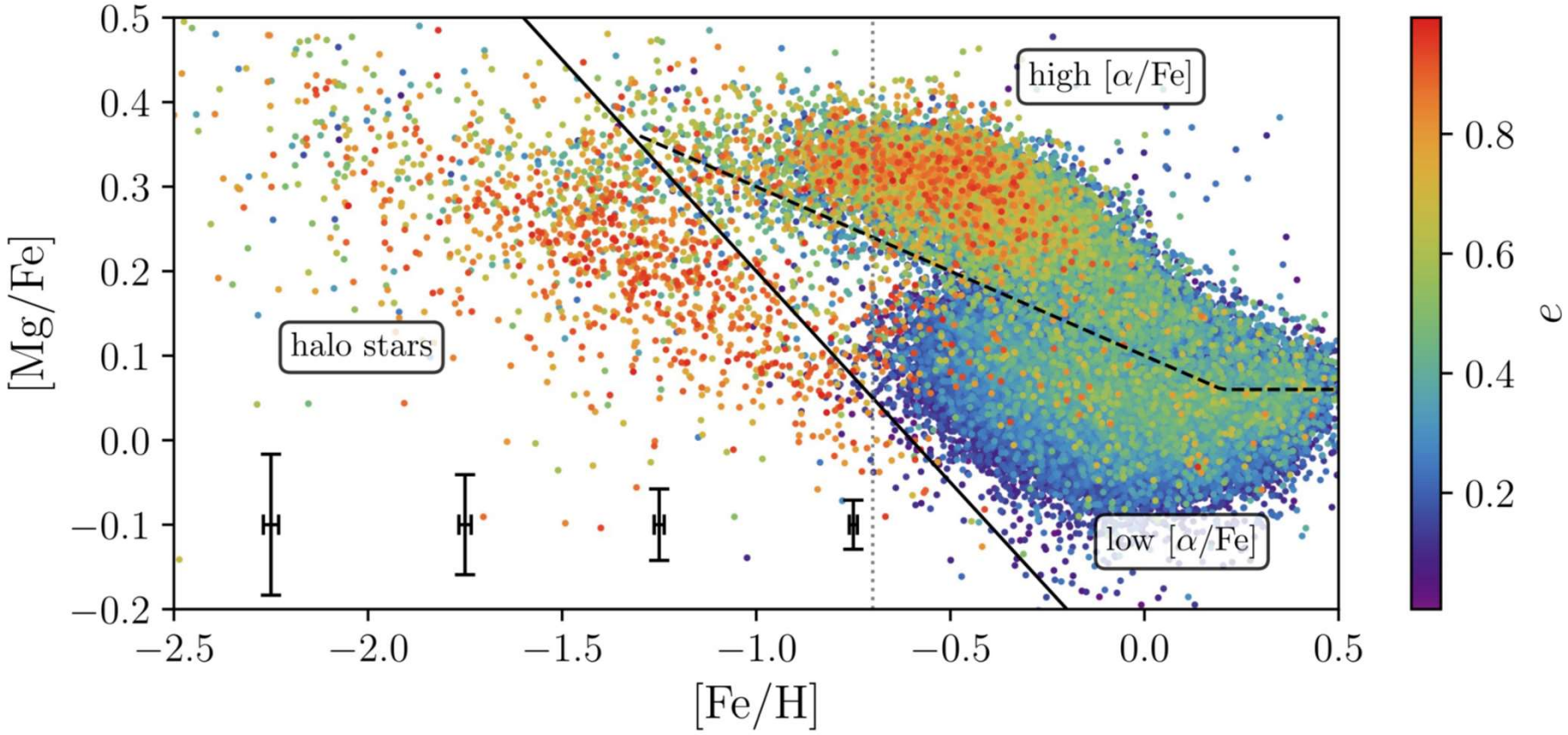

Duality (2-halos) in [α/Fe] ratios of halo stars

(Nissen & Schuster 2010)

High velocity stars =~ halo stars

$| V^{tot}_{star} - V_{LSR} | > 180$ km/s

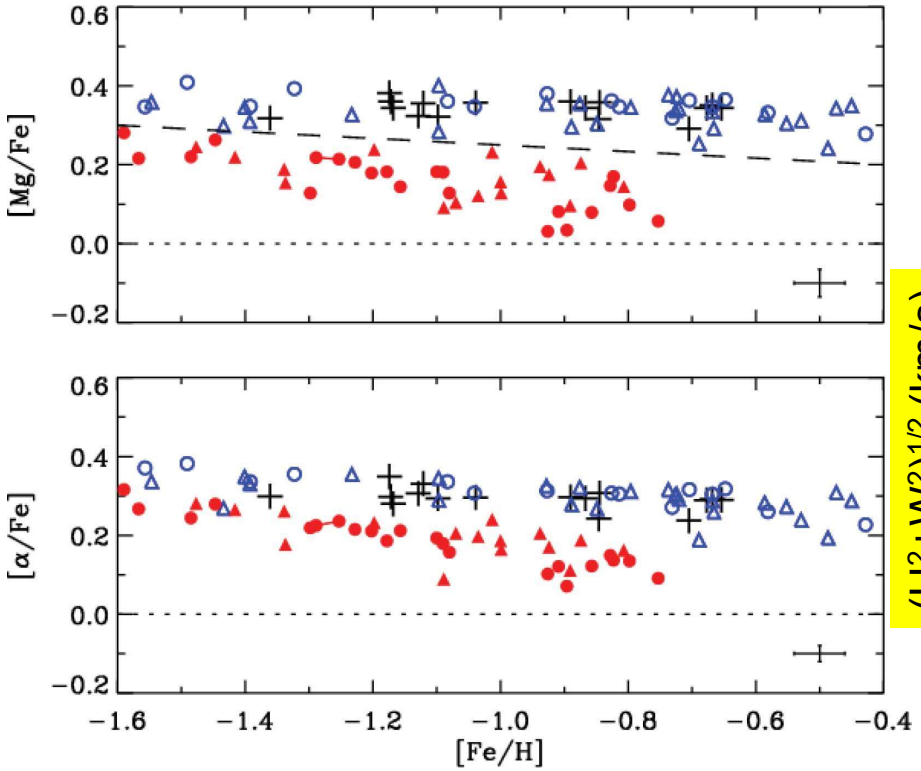

Blue: high-α stars

→ inner (in situ) halo?

Red: low-α stars

→ outer (ex situ) halo?

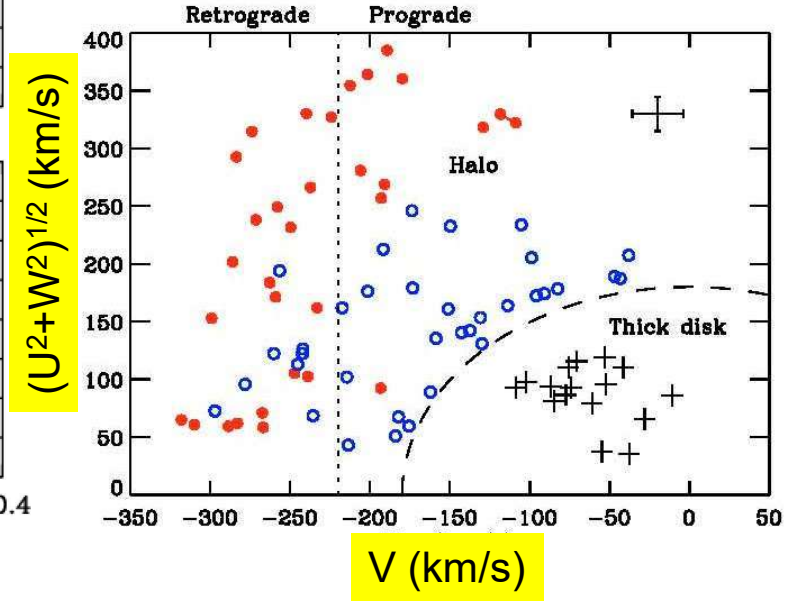

Based on VLT/UVES & NOT/FIES spectra

High-precision calibration with Δ= 0.02 ~ 0.04 dex

[Al/Fe] for accreted (low α)/canonical (high α) halo

Hawkins et al. 2015 for $-1.20 < [Fe/H] < -0.55$ (APOGEE DR12)

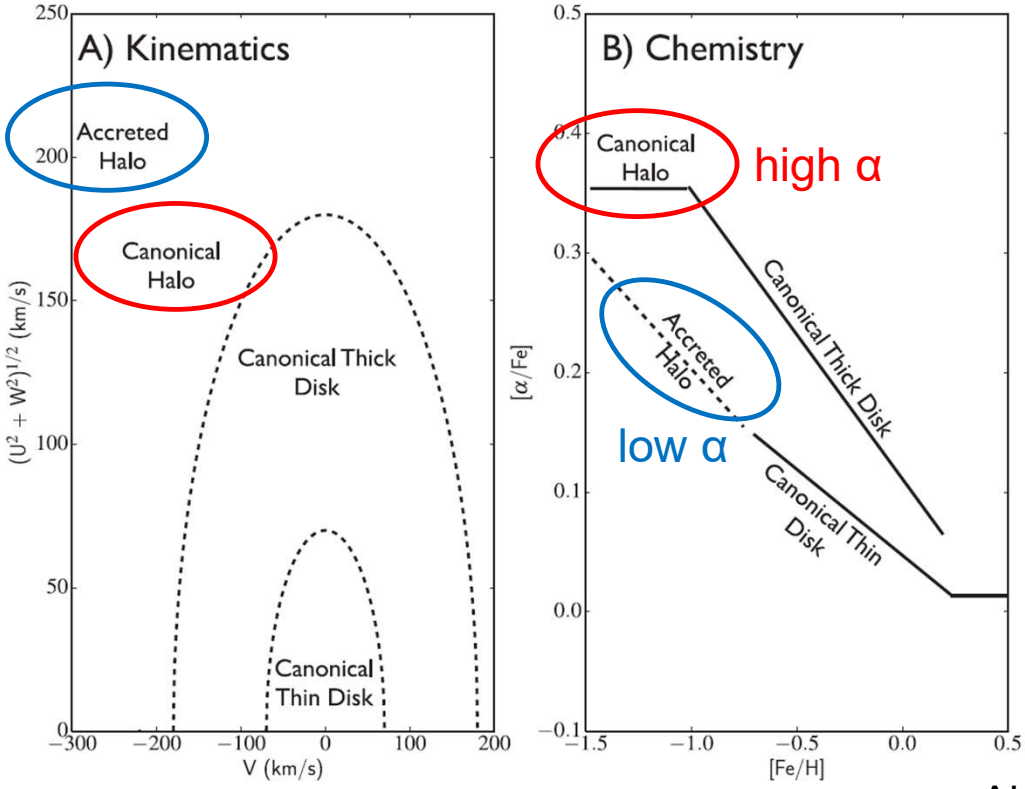

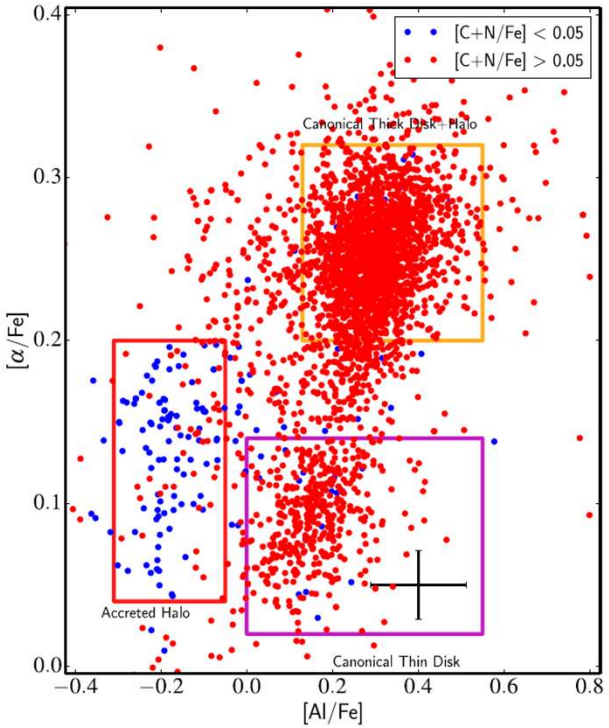

Al from SNII and is sensitive to initial C+N abundance

U
(V_R)

V
(V_Φ-V_{LSR})

W
(V_Z)

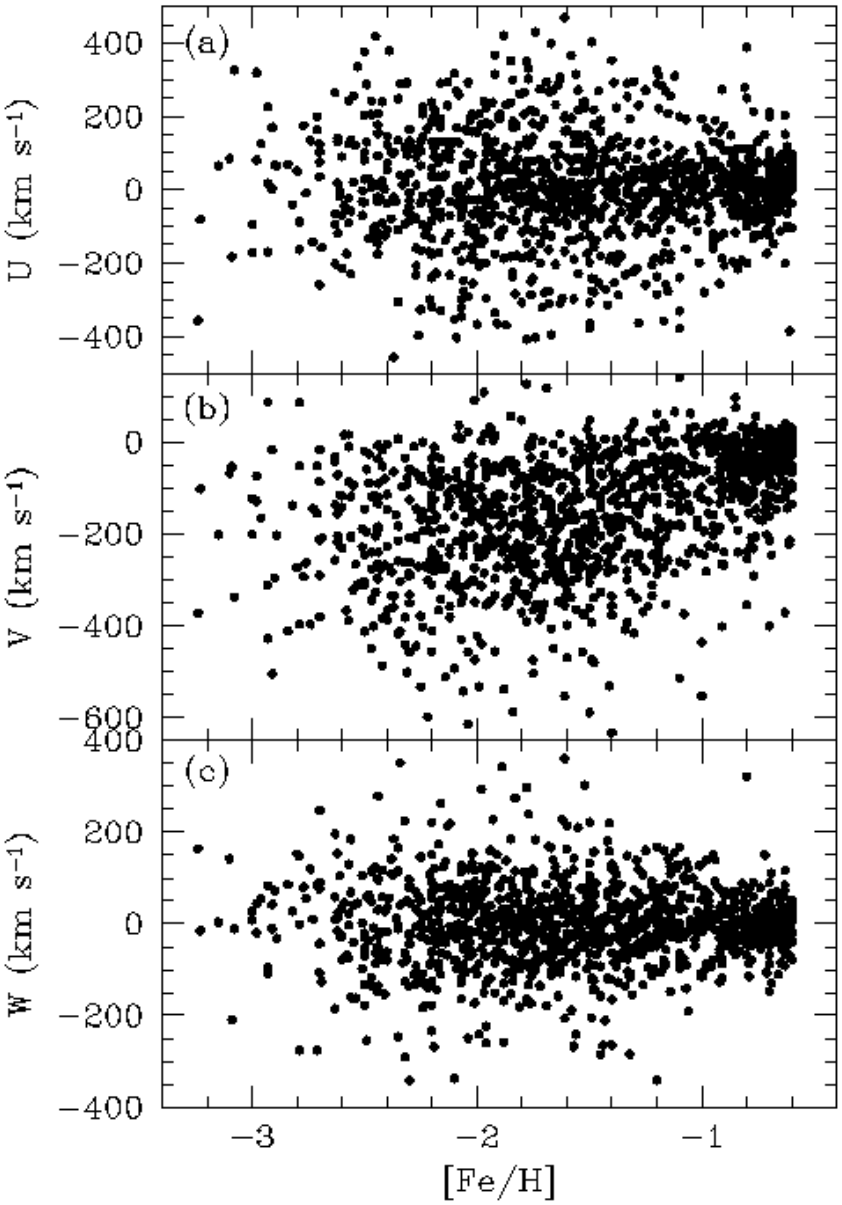

3D velocities of nearby 1203 stars using Hipparcos Catalog
(Chiba & Beers 2000)

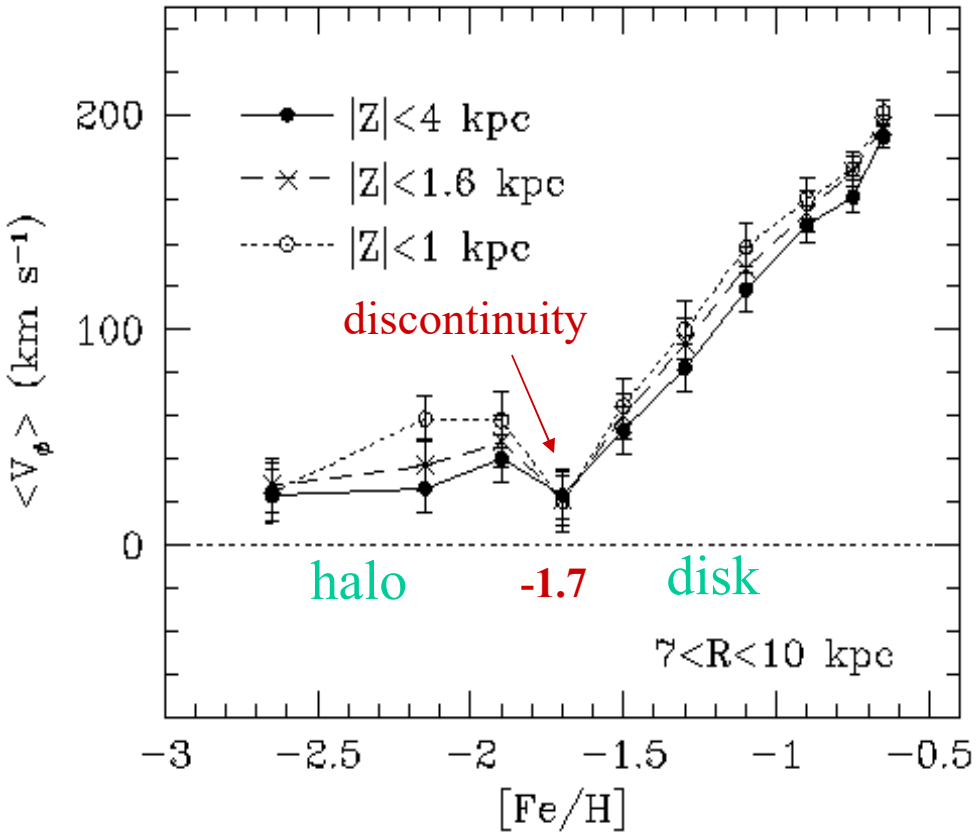

Velocity distribution of nearby stars

Sloan Digital Sky Survey

(Carollo et al. 2007, 2010)

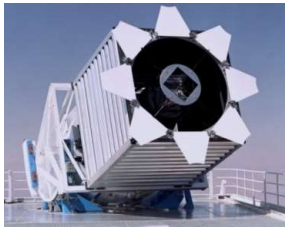

V_R (km/s)

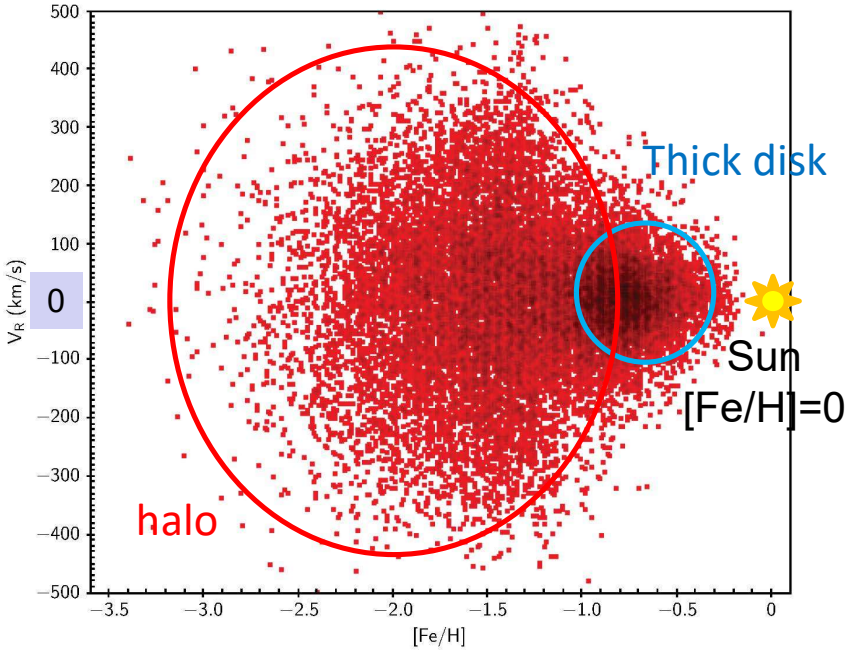

[Fe/H]

V_ϕ (km/s)

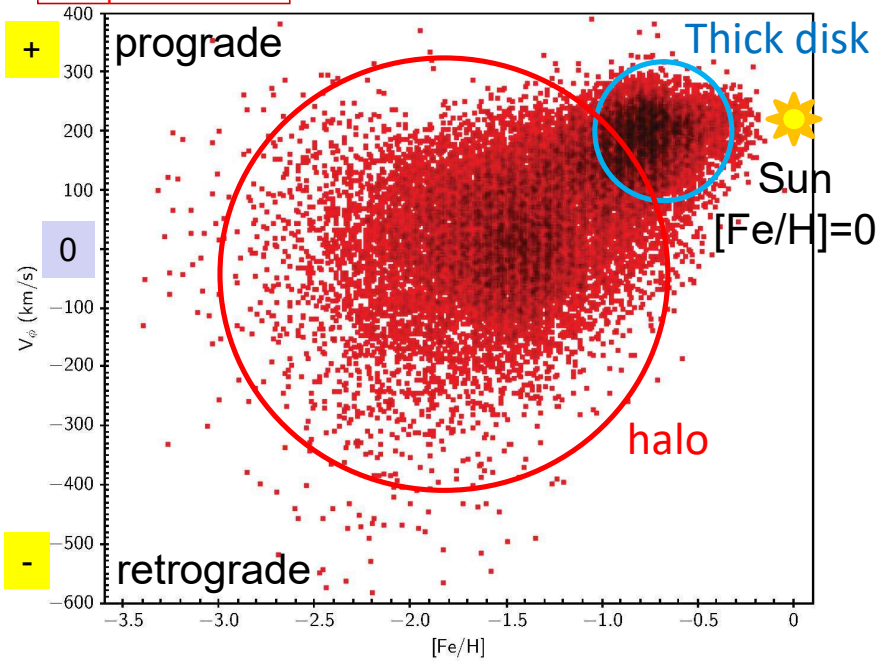

[Fe/H]

Result using Gaia: Belokurov et al. 2018
Elongated toward Vr: Sausage-like feature in halo stars

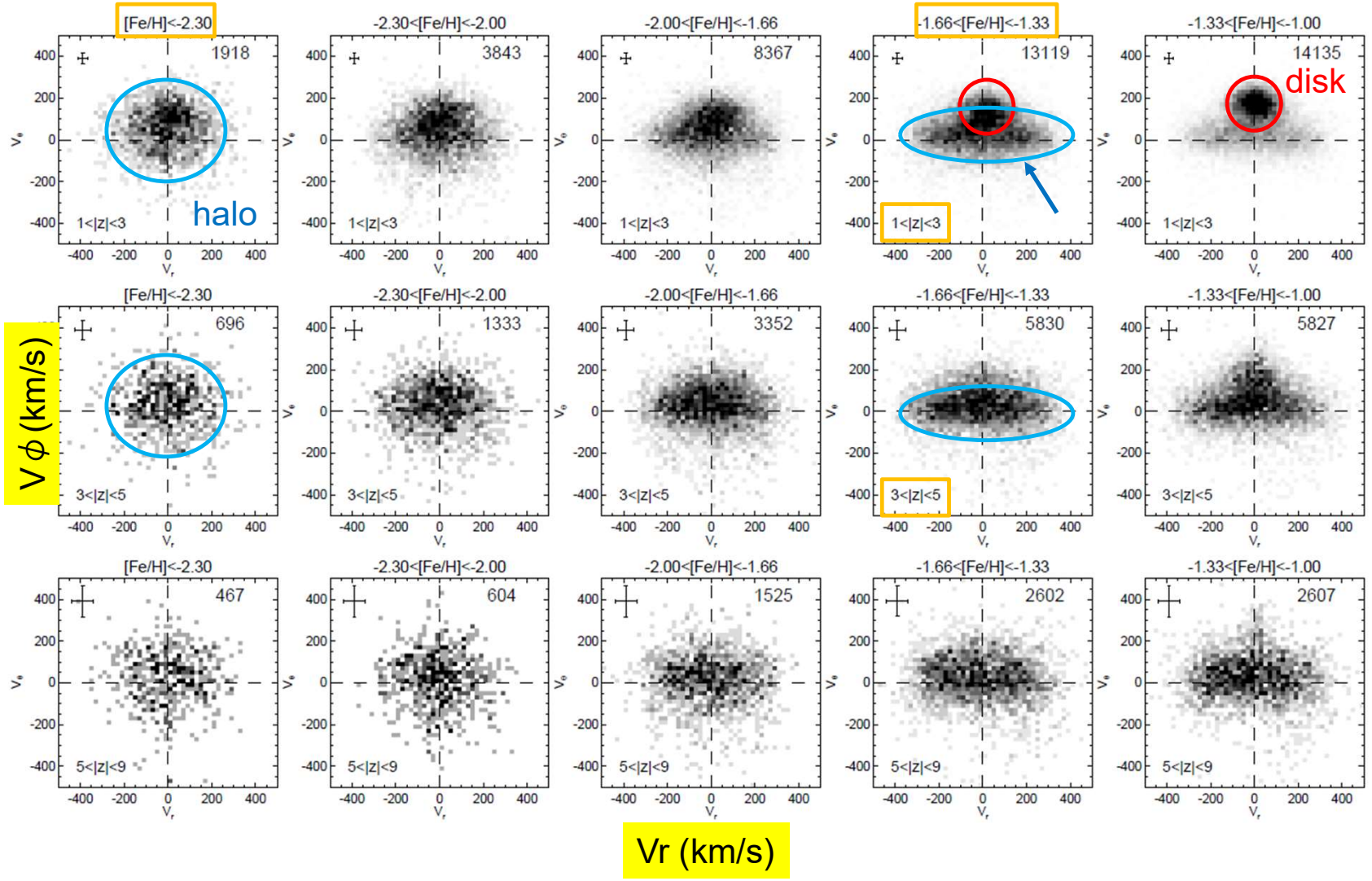

Nearby stars in (E,L_z,I_3) phase space
SDSS-DR7 Calibration Stars + Gaia DR2

Carollo & Chiba 2021, ApJ, 981, 191

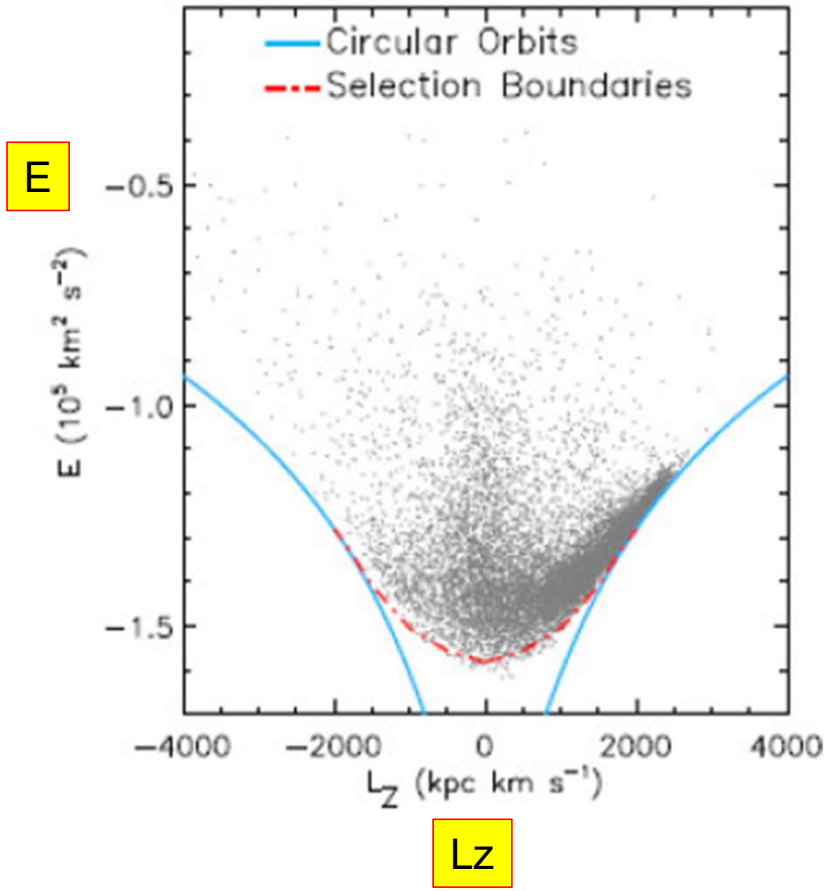

(R,z) distribution
of sample stars

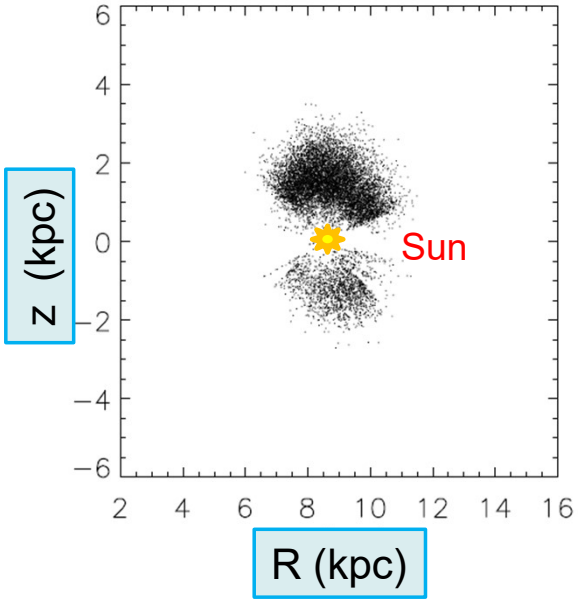

(E,Lz,I_3) space fromSDSS-DR7 Calibration Stars + Gaia DR2 Carollo & Chiba 2021

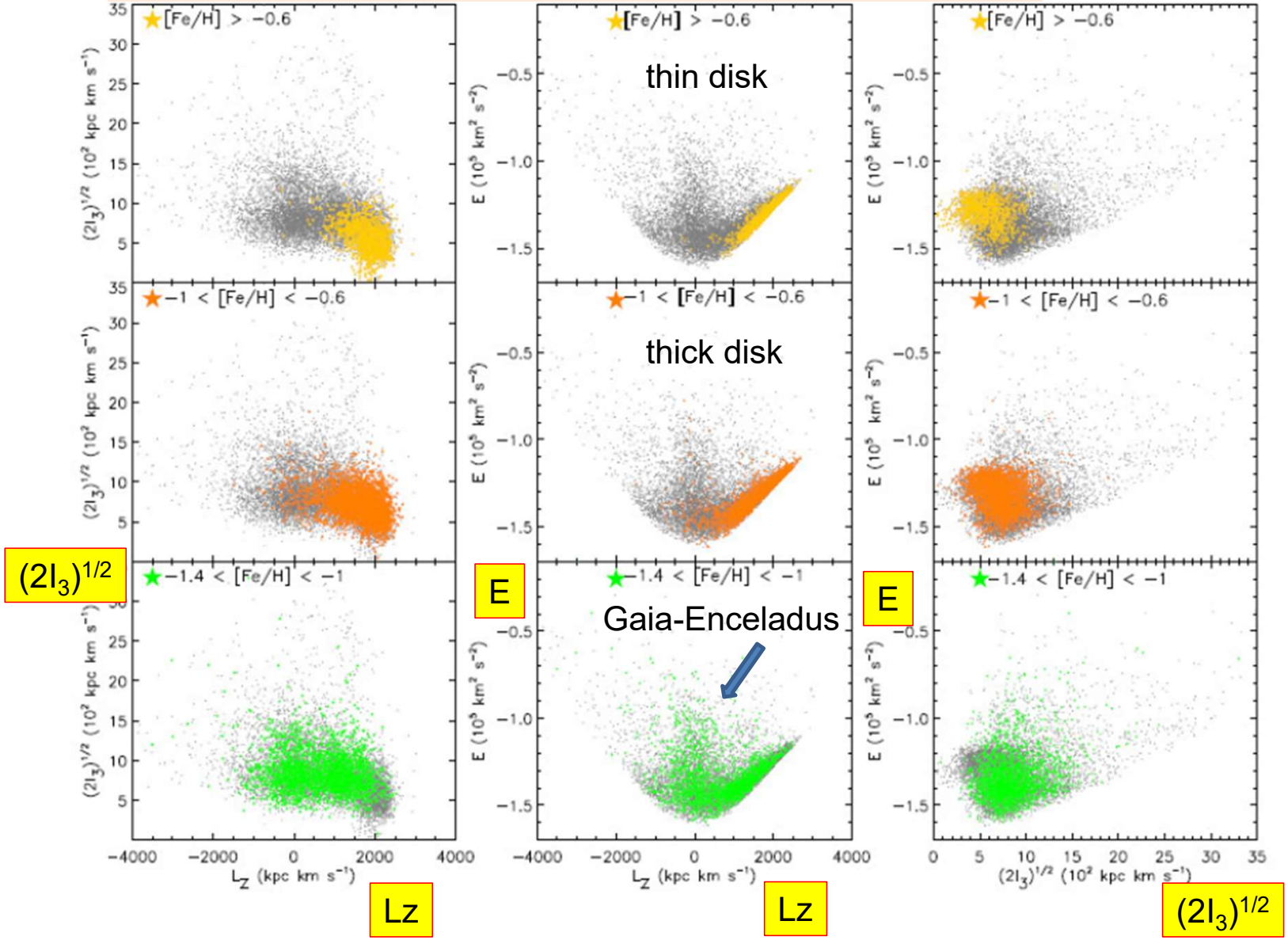

(E,Lz,I_3) space fromSDSS-DR7 Calibration Stars + Gaia DR2 Carollo & Chiba 2021

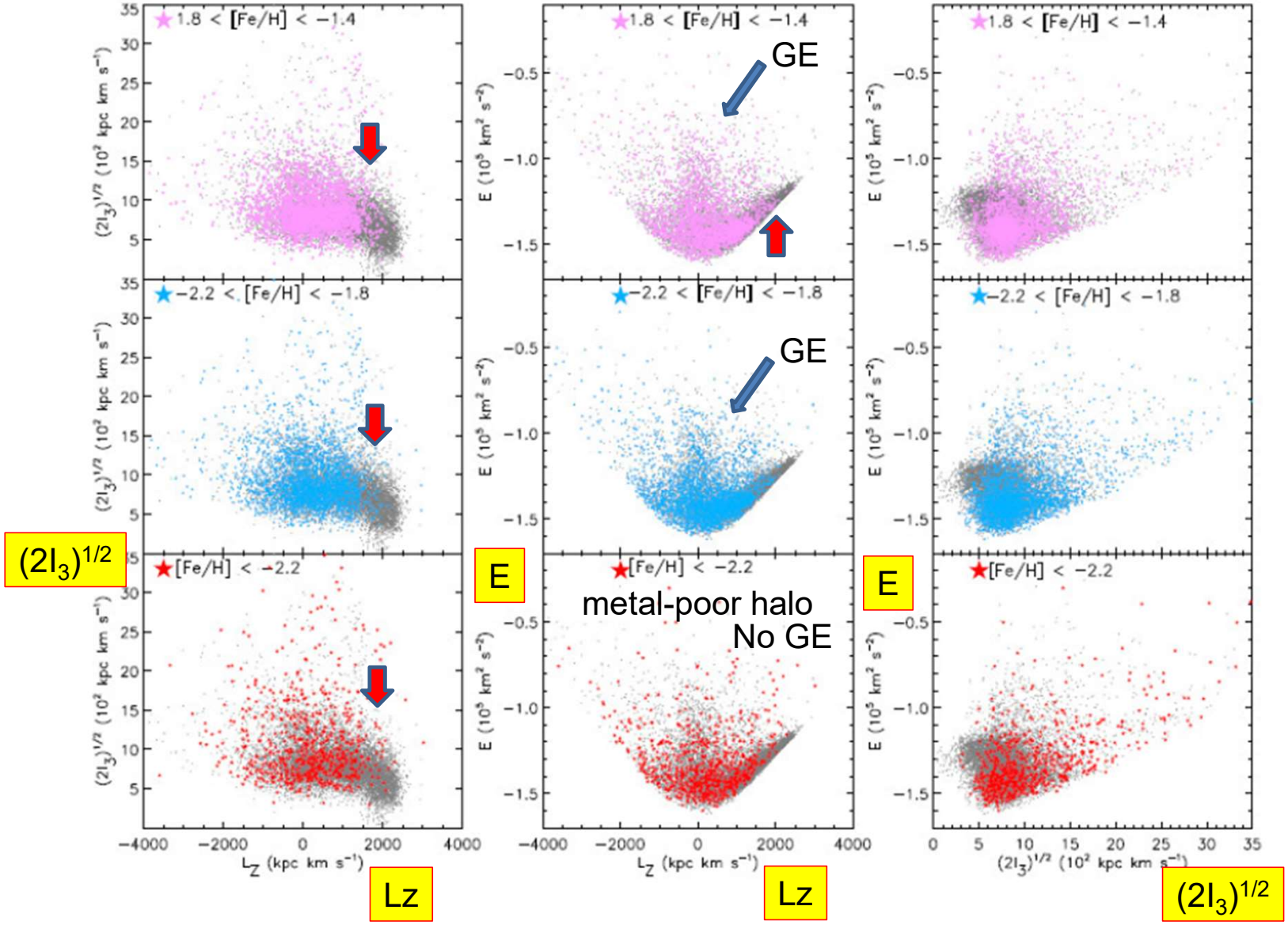

Comparison with abundance ratios

SDSS-DR7 Calibration Stars + Gaia DR2

Carollo & Chiba 2021

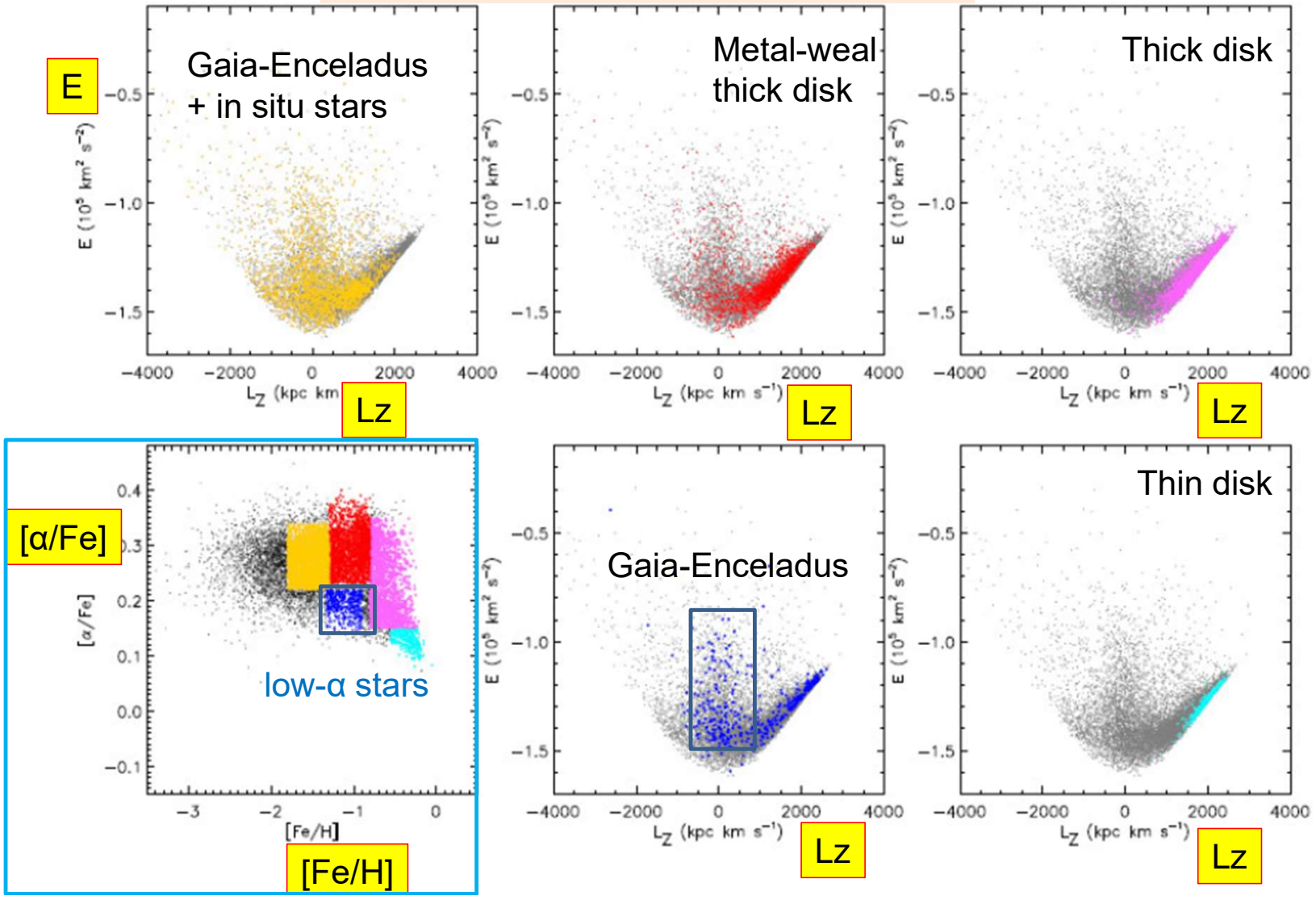

3.4 Globular clusters

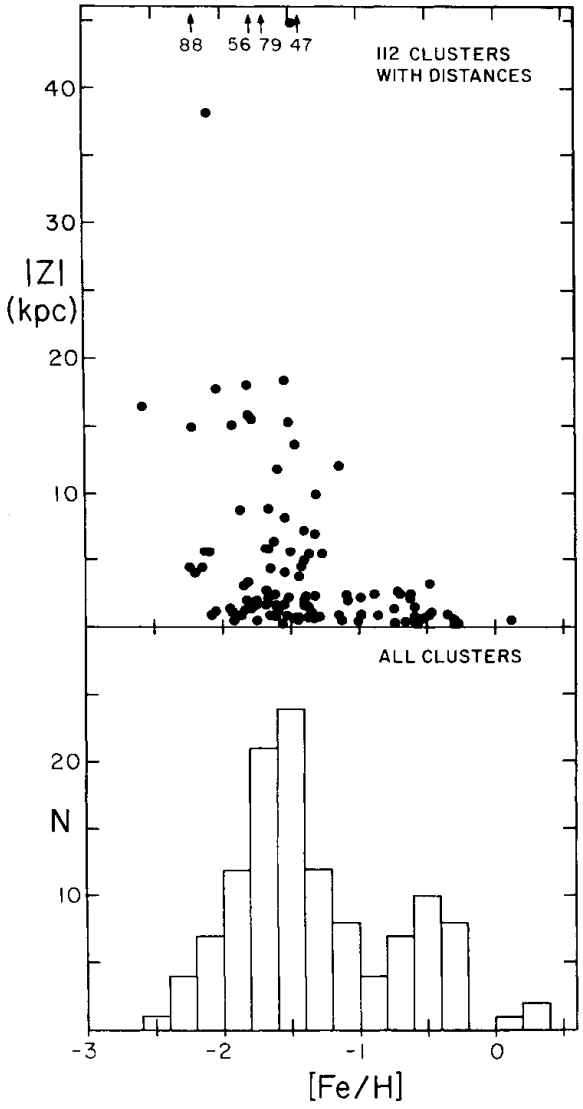

Zinn 1985, ApJ, 293, 424

Halo clusters, disk (bulge) clusters

Zinn 1993, ASP Conf. vol.48

HB morphology

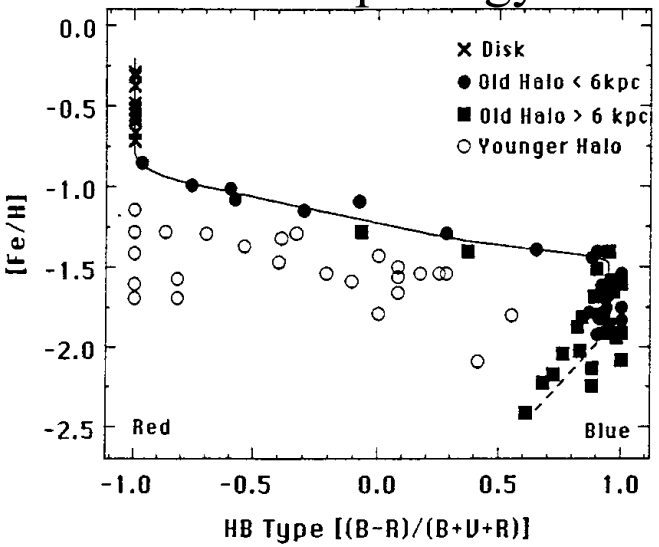

Fig. 1. The subdivision of the halo clusters ([Fe/H] < -0.8). The lines have been placed through the "Old Halo" clusters. The "Younger Halo" clusters lie more than 0.4 in HB type, at constant [Fe/H], to the left of the lines.

HB type (color) vs. metallicity in Galactic globular clusters

Mackey & Gilmore 2004, MN, 355, 504

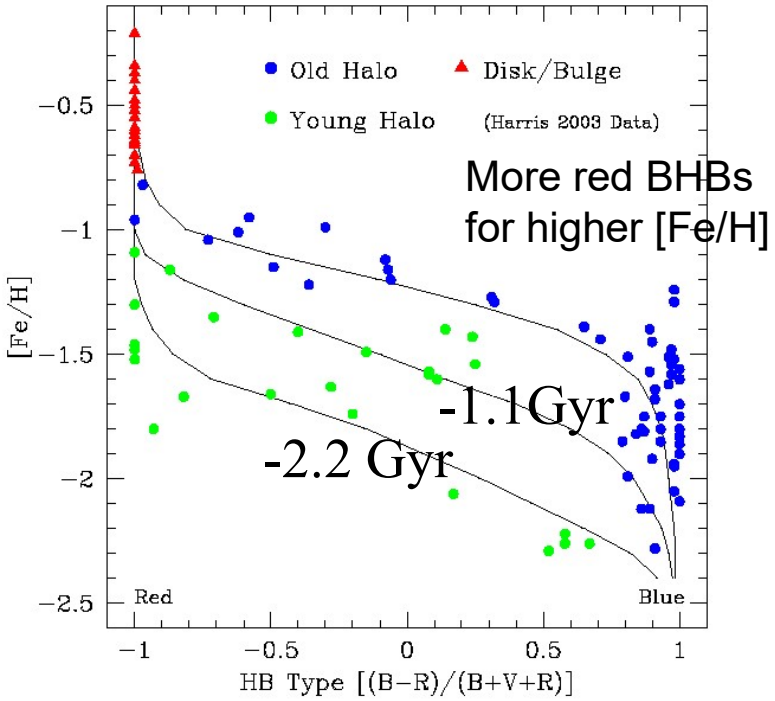

Figure 5. HB-type versus metallicity diagram for the 108 Galactic globular clusters with suitable measurements in the Harris (1996) catalogue. The clusters have been divided into three subsystems, as labelled, according to criteria very similar to those of Zinn (1993a). The overplotted isochrones are from Rey et al. (2001) and constitute the latest versions of the Lee et al. (1994) synthetic HB models. The two lower isochrones are, respectively, 1.1 Gyr and 2.2 Gyr younger than the top isochrone.

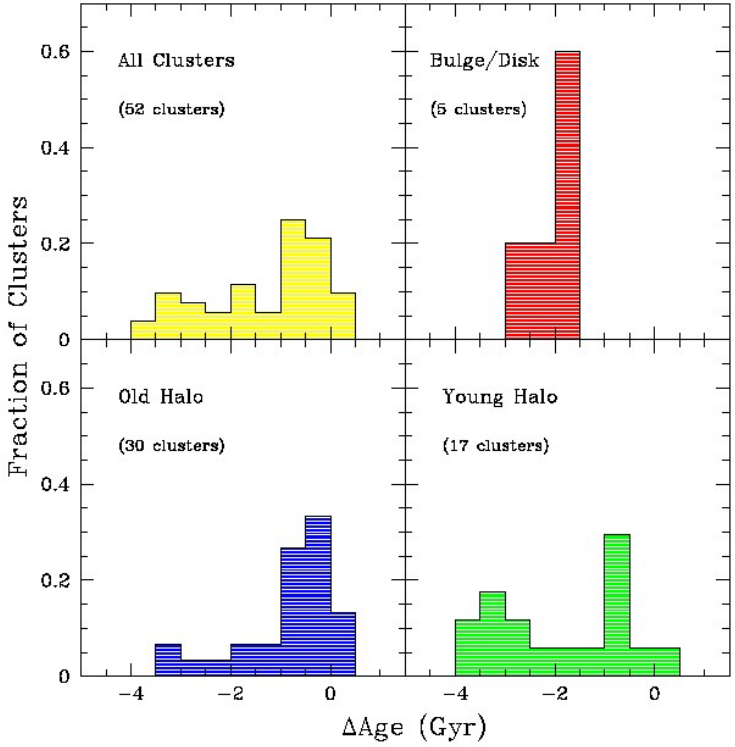

Figure 9. Histograms of ages for 52 Galactic globular clusters, as labelled The ages are taken from Salaris & Weiss (2002), calculated relative to the age of M92 as described in the text.

Relative to the age of M92
(~ 12.6 Gyr)

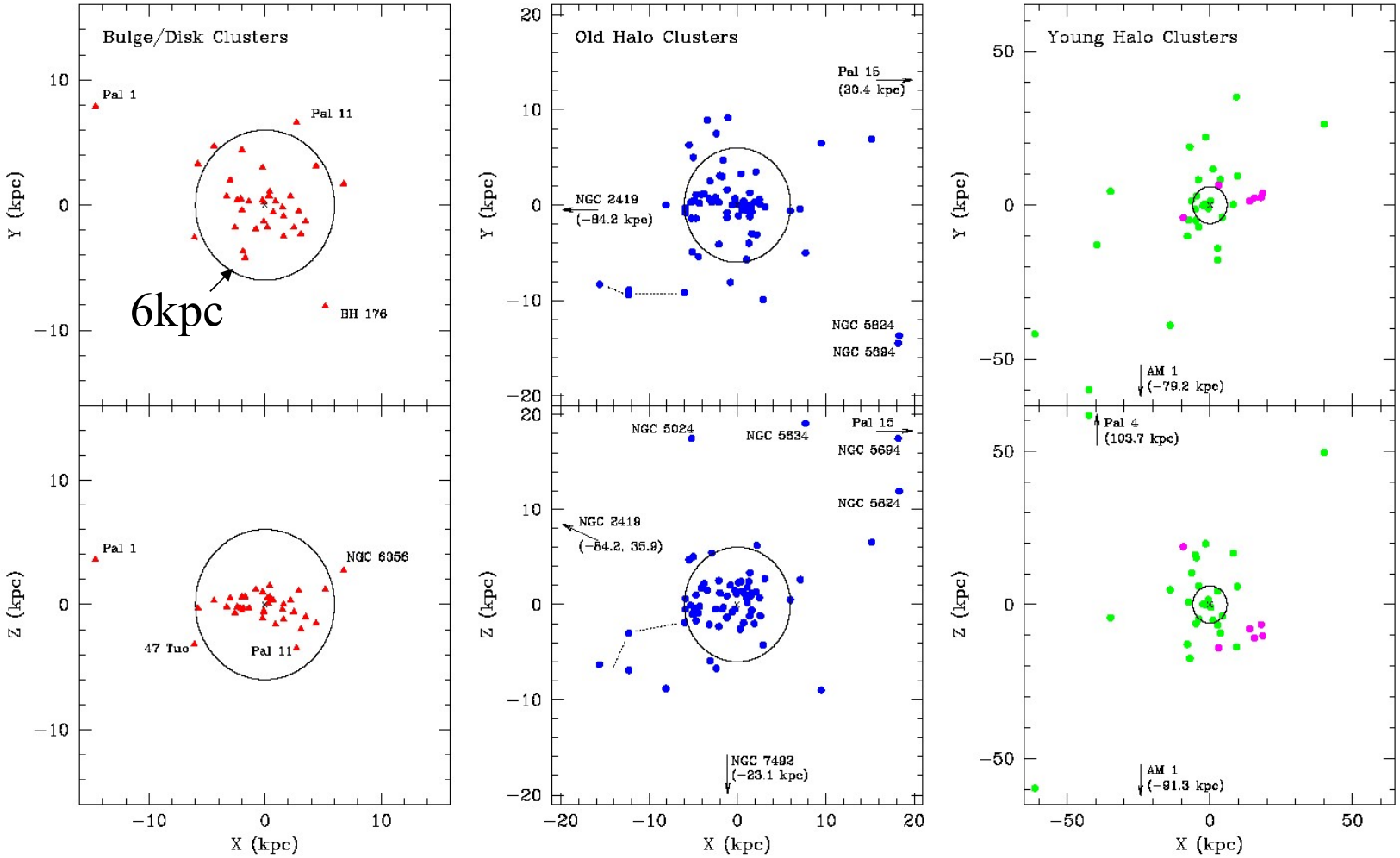

Figure 7. Spatial positions of globular clusters in each of the Galactic subsystems, as labelled, in Galactocentric Cartesian coordinates. In this system the Sun is at $(X, Y, Z) = (-8, 0, 0)$. In each diagram a circle of radius 6 kpc is marked. This helps give an indication of the relative volumes occupied by the three systems. Clusters discussed at various points in the text are labelled, as are those objects which fall outside the range of a given plot. The six Sagittarius clusters are marked with open circles (magenta points in the electronic version of the figure) in the young halo diagram, while the four clusters linked with the Canis Major dwarf – NGC 1851, 1904, 2298 and 2808 (Martin et al. 2004) – are joined with a dotted line in the old halo plot.

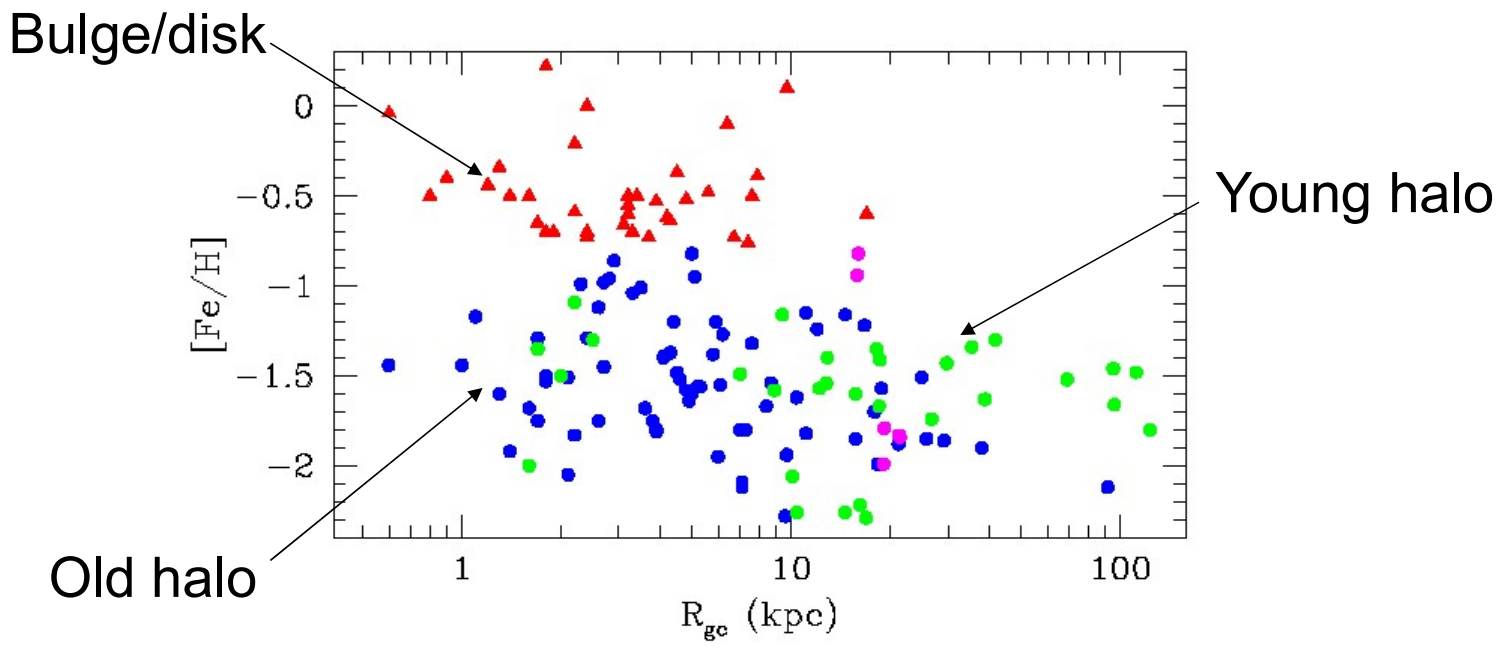

Figure 8. Metallicity versus Galactocentric radius for the three Galactic globular cluster subsystems, plus the Sagittarius clusters. Measurements are taken from the Harris (1996) data base, except for the Sagittarius clusters, which have measurements compiled in Tables 2 and 3. The bulge/disc clusters are solid triangles (red in the electronic version), while the old halo clusters are solid dots (blue dots in the electronic version), the young halo clusters are open circles (green solid dots), and the Sagittarius clusters are asterisks (magenta solid dots).

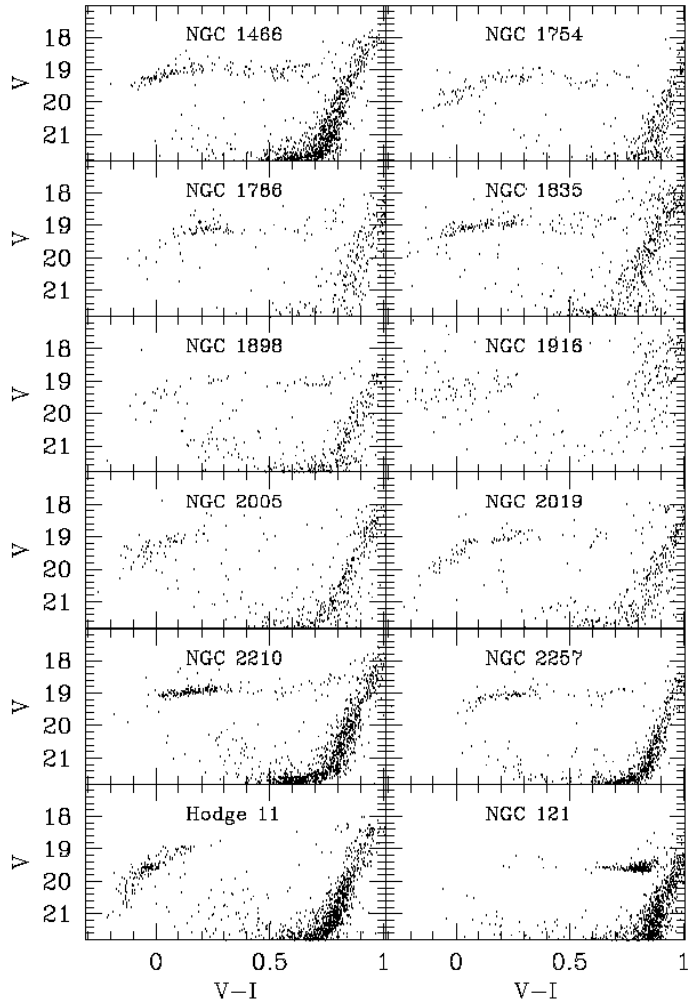

Figure 3. Colour–magnitude diagrams showing the horizontal branches for 12 of the old LMC and SMC clusters from Fig. 1. The photometry has been corrected for reddening using the literature values from Table 2. For targets badly affected by field star contamination (NGC 1754, 1786, 1835, 1898, 1916, 2005, 2019), only stars within 10 arcsec of a given cluster centre are plotted. For the remaining clusters, only stars within 50 arcsec of a given centre are plotted.

Clusters in the LMC, SMC, + Fornax and Sgr dwarf galaxies

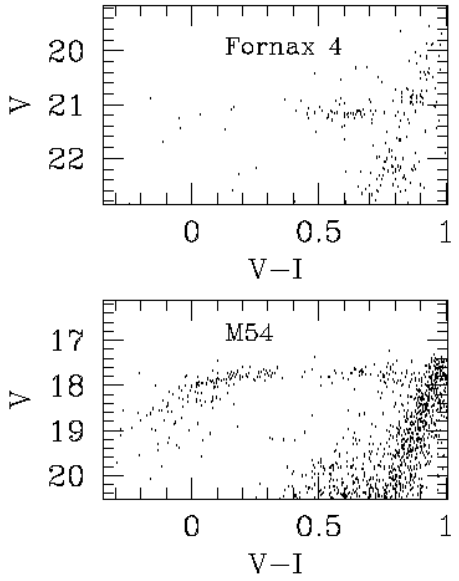

Figure 4. Colour–magnitude diagrams showing the horizontal branches of Fornax 4 (upper) and M54 (lower). The photometry has been corrected for reddening using the literature values from Table 2. For Fornax 4, only stars within 12 arcsec of the cluster centre are plotted, while for M54, only stars within 25 arcsec of the centre are plotted.

LMC

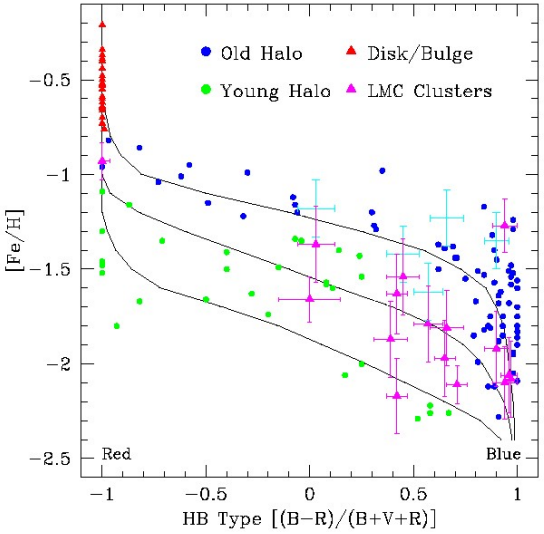

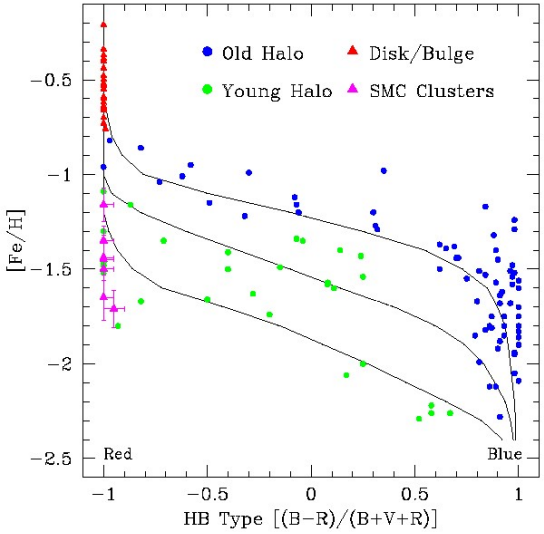

SMC

Fornax

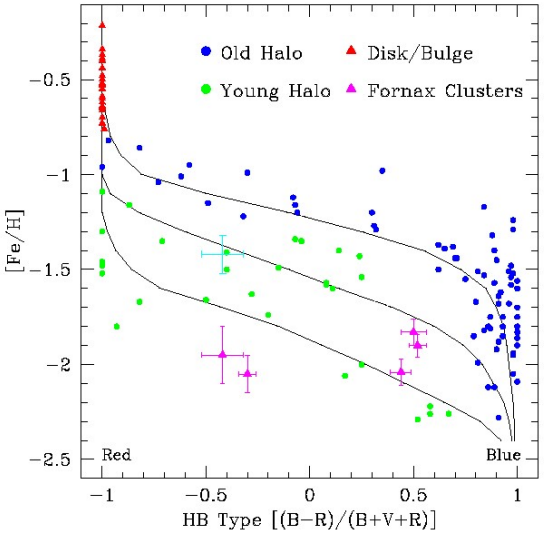

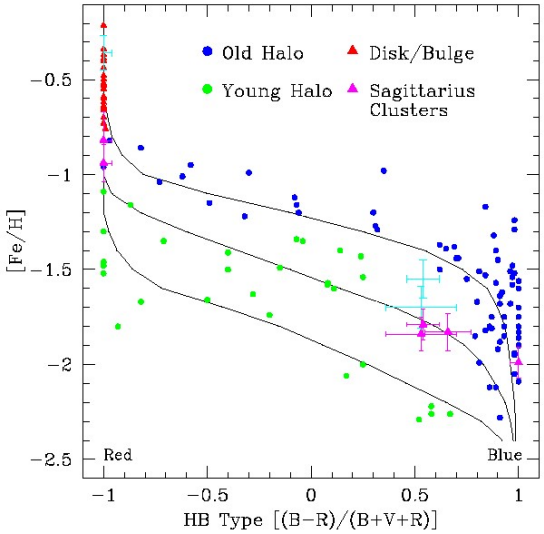

Sagittarius

Figure 13. HB-ty … lower right) cluster systems. Po … e electronic version) represent … chrones are as in Fig. 6 – with the two lower isochrones, respectively, 1.1 Gyr and 2.2 Gyr younger than the top isochrone.

Young halo clusters → external origin!?

EHB:
Extended HB

ω Centauri
Lee et al. 1999

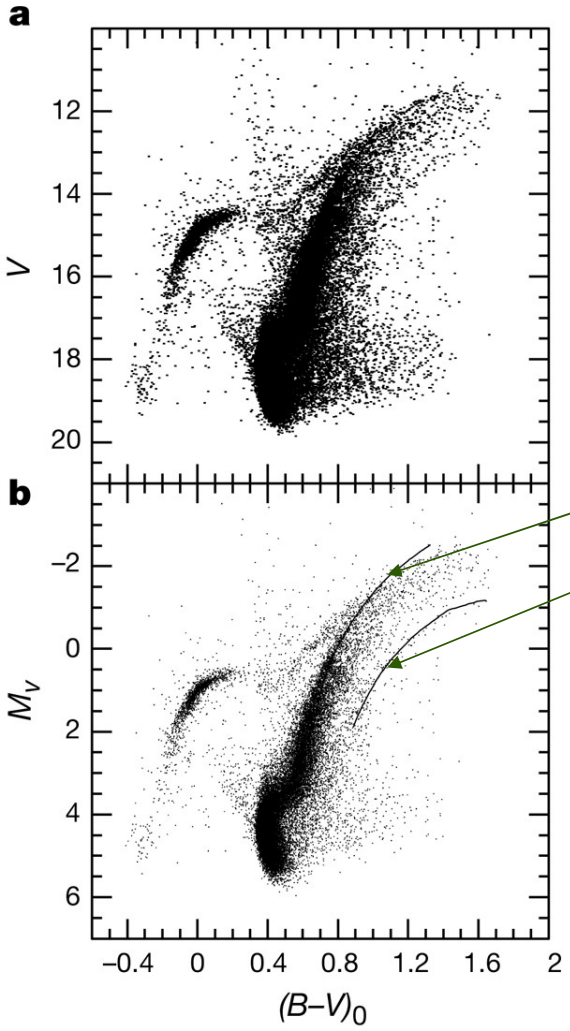

CTIO 0.9m

Z=0.0004
0.005

ω Centauri
Bedin et al. 2004

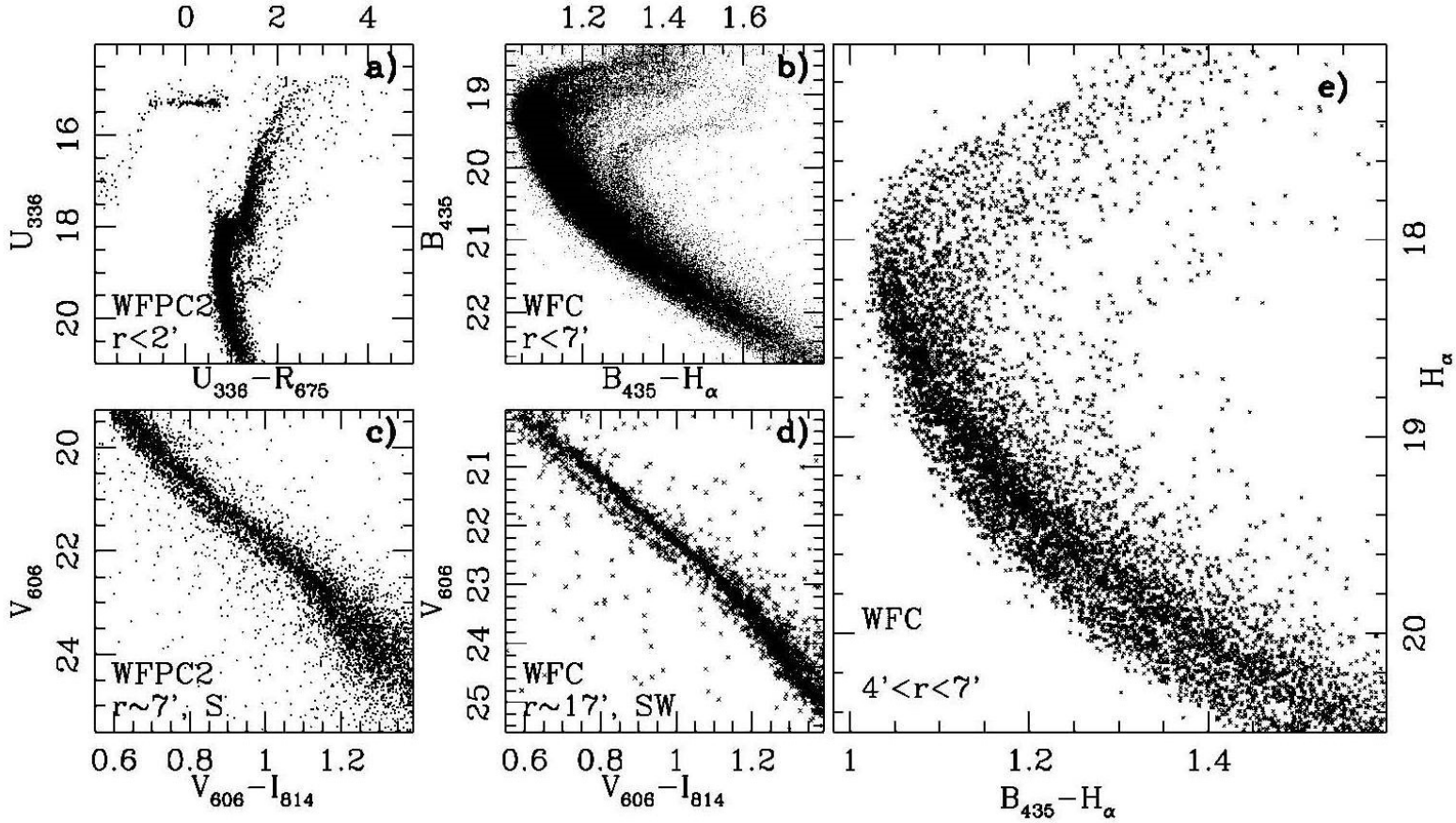

High helium abundance !?
Norris 2004

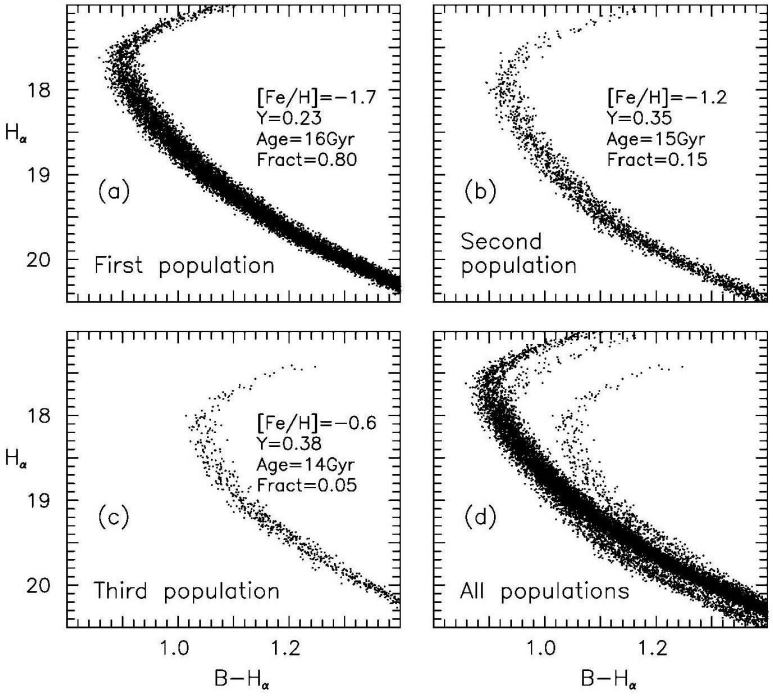

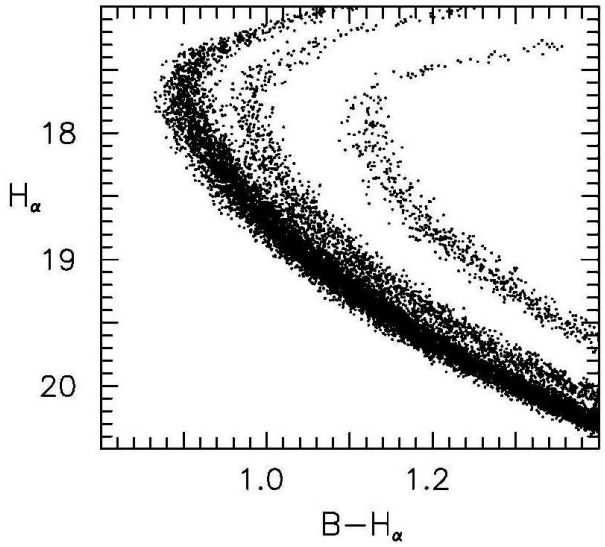

FIG. 3.—Synthetic composite CMD of the main sequence of ω Cen computed for the population fractions, Z, and ages in Table 1, but with all populations having $Y = 0.23$.

THE THREE POPULATIONS OF ω CEN

Population (1)	Fraction (2)	[Fe/H] (3)	Z (4)	Y (5)	Age (Gyr) (6)
First	0.80	−1.7	0.00040	0.23	16
Second	0.15	−1.2	0.00126	0.35	15
Third	0.05	−0.6	0.00502	0.38	14

Na-O anti-correlation in GCs

(Carretta+ 2010)

general properties of GCs ⇒ multiple stellar population!?

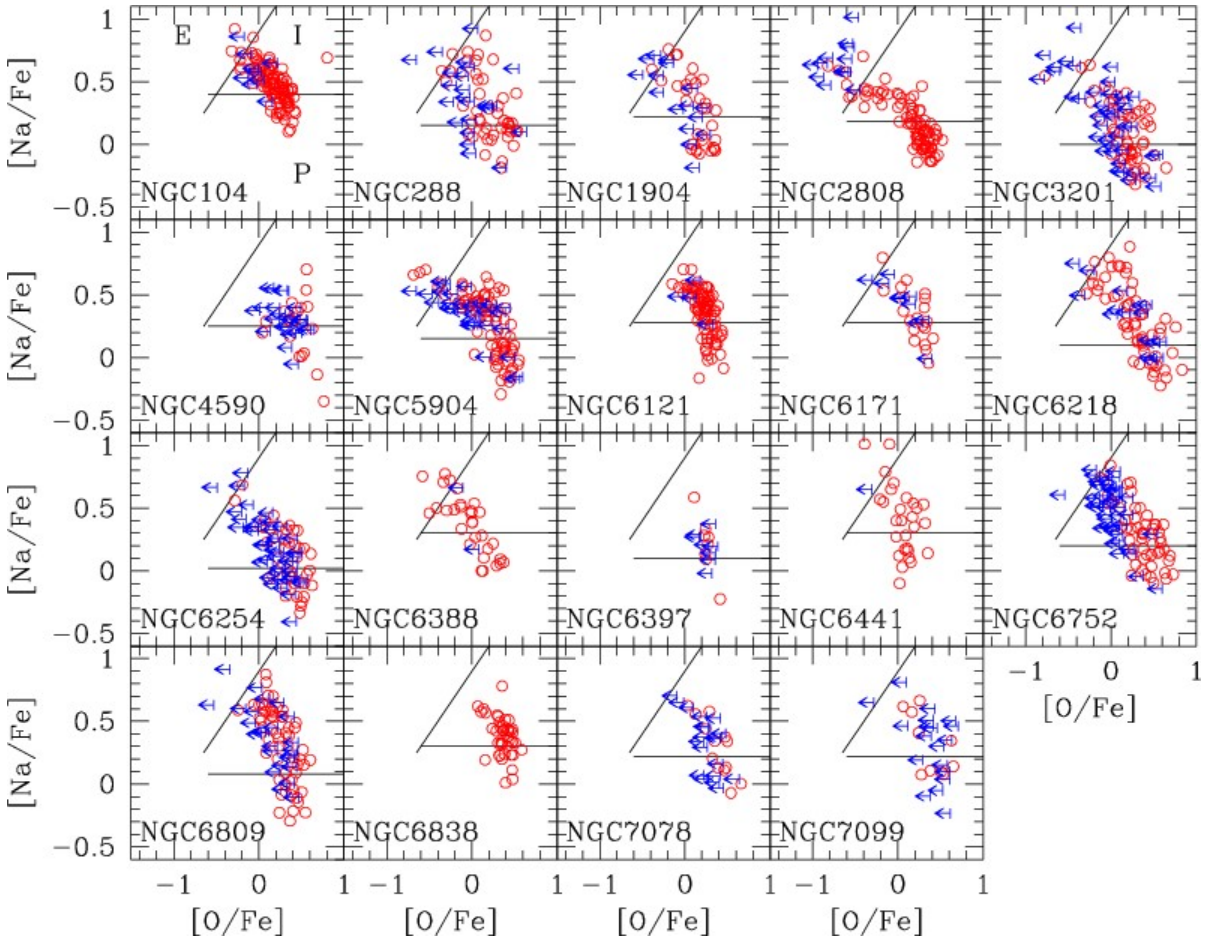

H-burning at high T
(CNO, NeNa,
MgAl cycle)

1. First-generation stars changed Na & O abundance inside these stars (Na⇑ O⇓)
2. Gas was expelled via. AGB & SN.
3. New-generation stars formed from this processed gas

3.5 Galactic satellites

List of bright satellites

Name	Type	l [deg]	b [deg]	$D_\odot$ [kpc]	$D_{\rm LG}$ [Mpc]	M_V [mag]	μ_V [mag/"^{2}]	$\langle$[Fe/H]$\rangle$ [dex]
Galaxy	S(B)bcI-II	0.00	0.00	8	0.47	−20.9	—	—
Sgr	dSph,N?	6.00	−15.00	28	0.47	−13.8	25.4	−1.0
LMC	IrIII-IV	280.46	−32.89	50	0.49	−18.5	20.7	−0.7
SMC	IrIV/IV-V	302.80	−44.30	63	0.49	−17.1	22.1	−1.0
UMi	dSph	104.95	44.80	69	0.44	−8.9	25.5	−2.2
Dra	dSph	86.37	34.72	79	0.44	−8.6	25.3	−2.1
Sex	dSph	243.50	42.27	86	0.52	−9.5	26.2	−1.7
Scl	dSph	287.54	−83.16	88	0.45	−9.8	23.7	−1.8
Car	dSph	260.11	−22.22	94	0.52	−9.4	25.5	−2.0
For	dSph	237.29	−65.65	138	0.46	−13.1	23.4	−1.3
Leo II	dSph	220.17	67.23	205	0.57	−10.1	24.0	−1.9
Leo I	dSph	225.98	49.11	270	0.63	−11.9	22.4	−1.5
Phe	dIrr/dSph	272.49	−68.82	405	0.60	−9.8	—	−1.8
NGC 6822	IrIV-V	25.34	−18.39	500	0.68	−16.0	21.4	−1.2

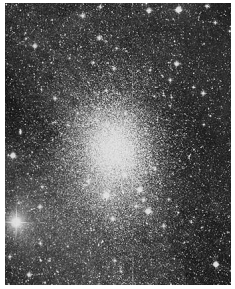

Scl

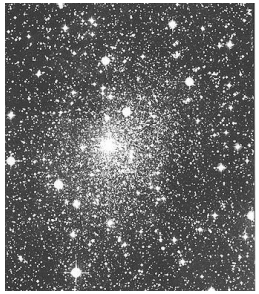

Car

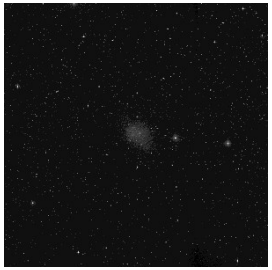

For

Leo II

Leo I

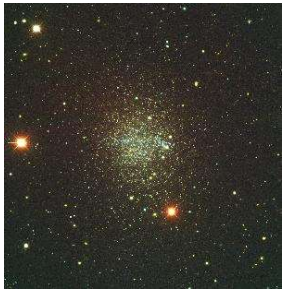

Phe

Milky Way & Galactic satellites

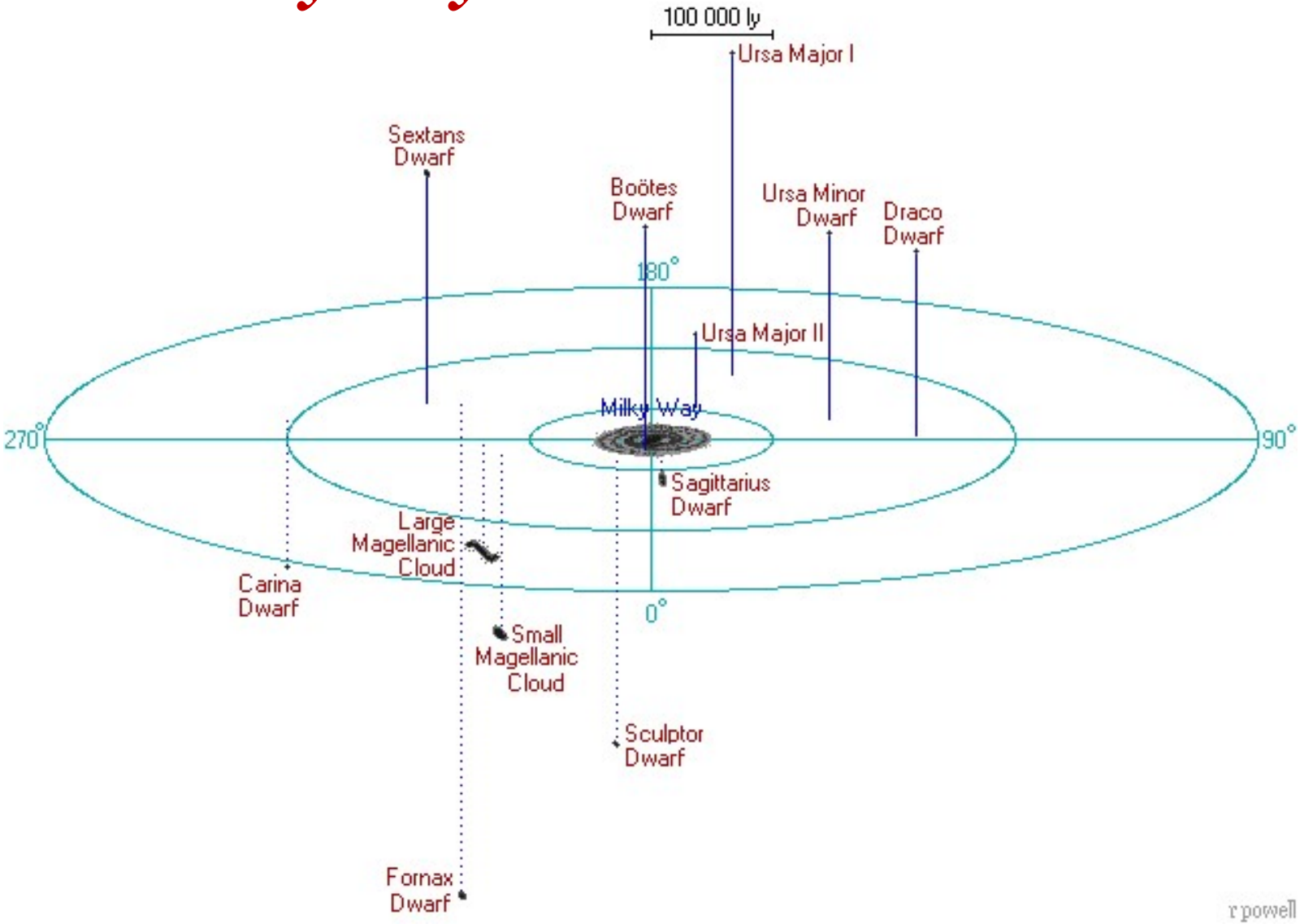

Fornax @ D=138 kpc

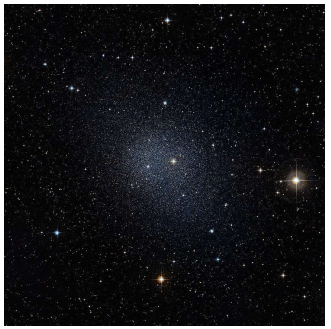

Buonanno+ 1999
(from HST image)

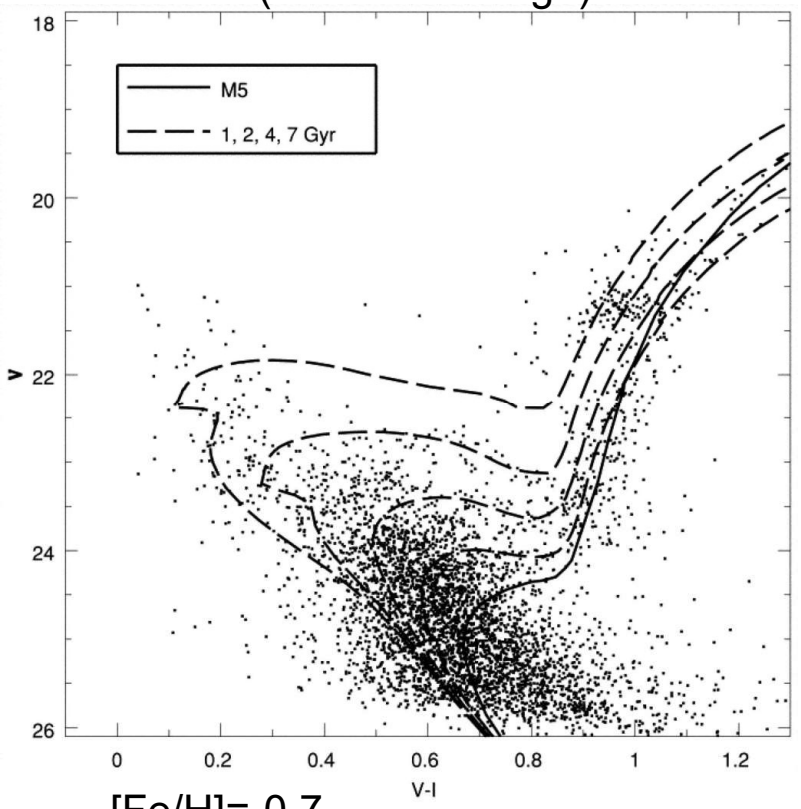

[Fe/H]=-0.7

de Boer+2012
(from CTIO image)

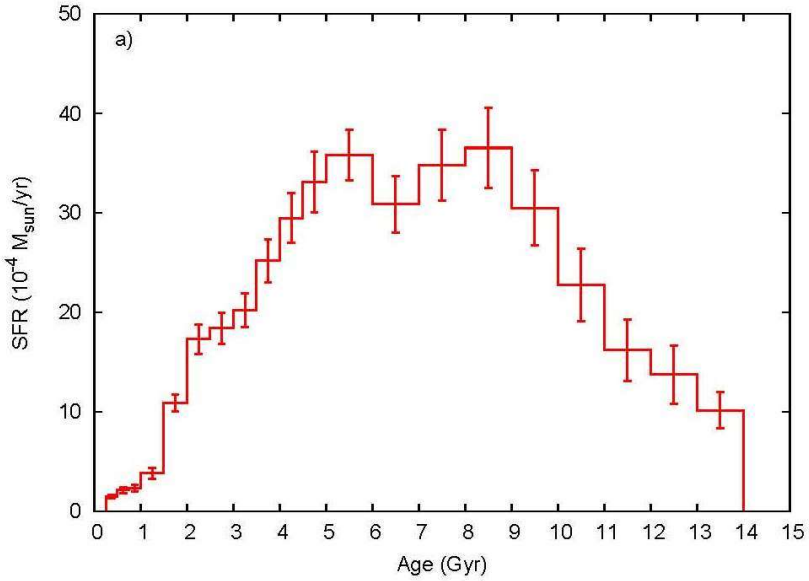

HST/WFPC2 results

(Weisz et al. 2014)

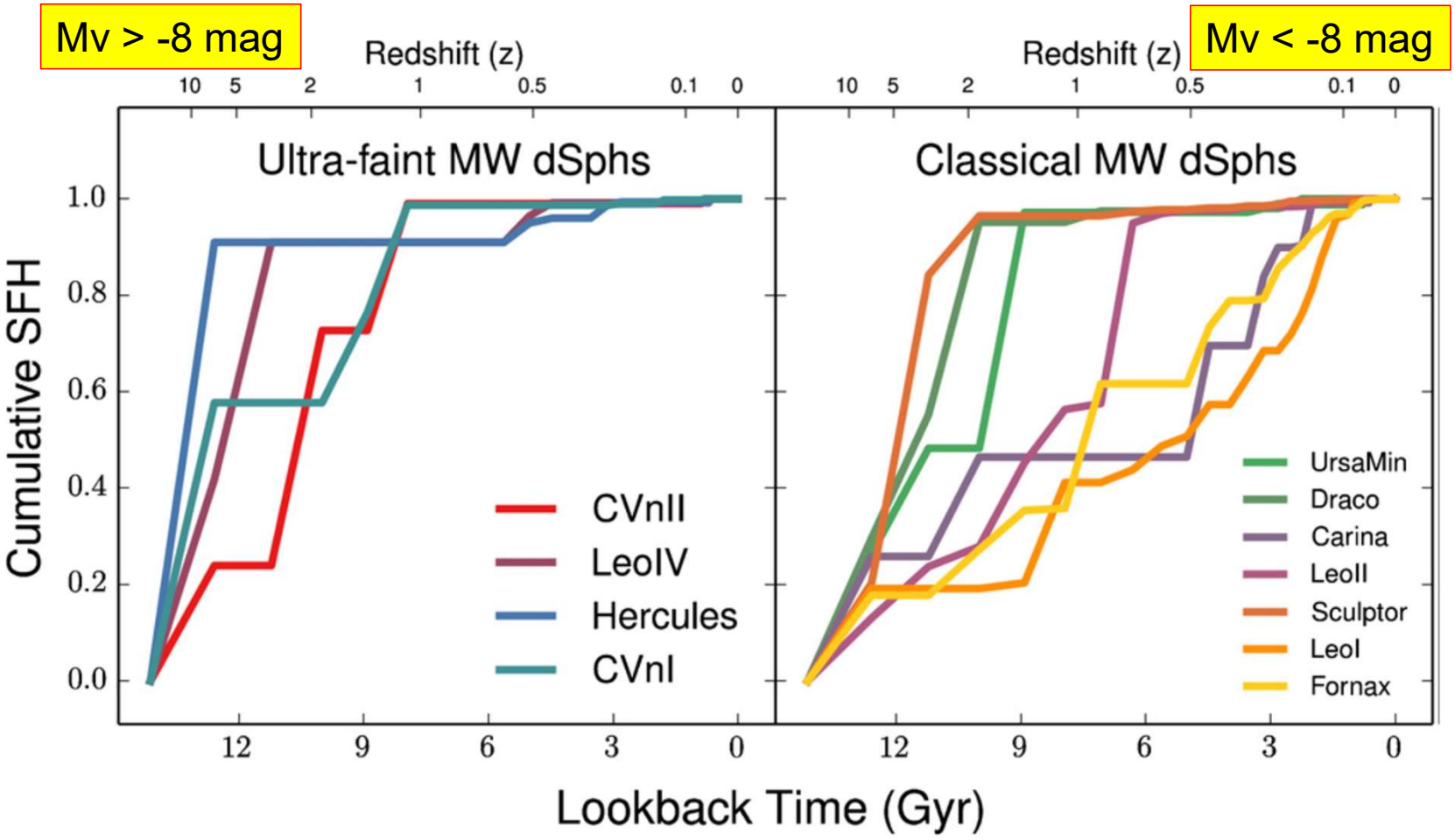

Keck/DEIMOS spectroscopic survey by Kirby+09,11

Sculptor

slit mask

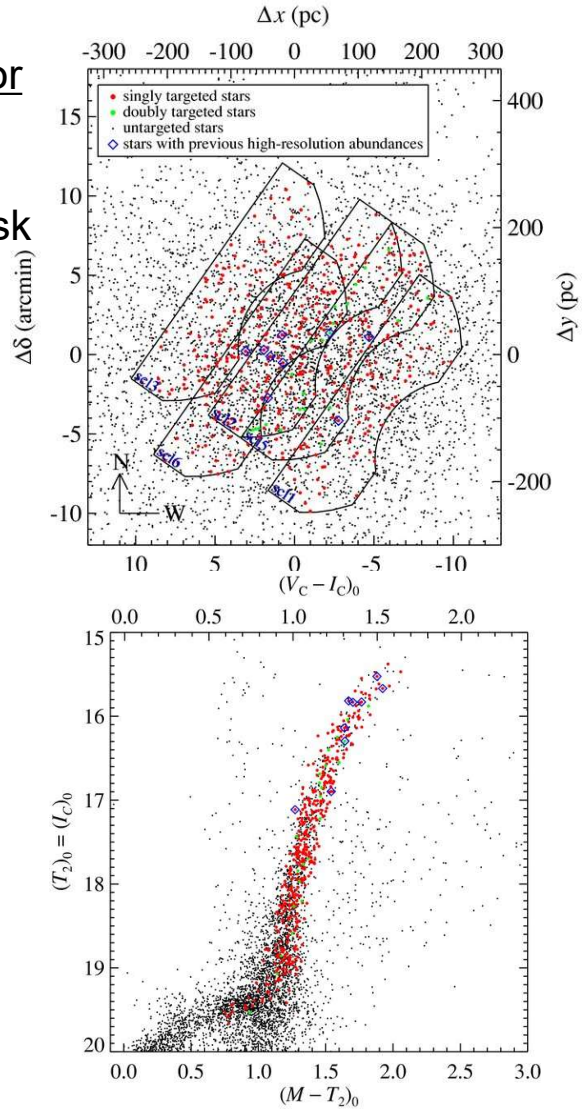

Metallicity Distribution Functions in several dSphs

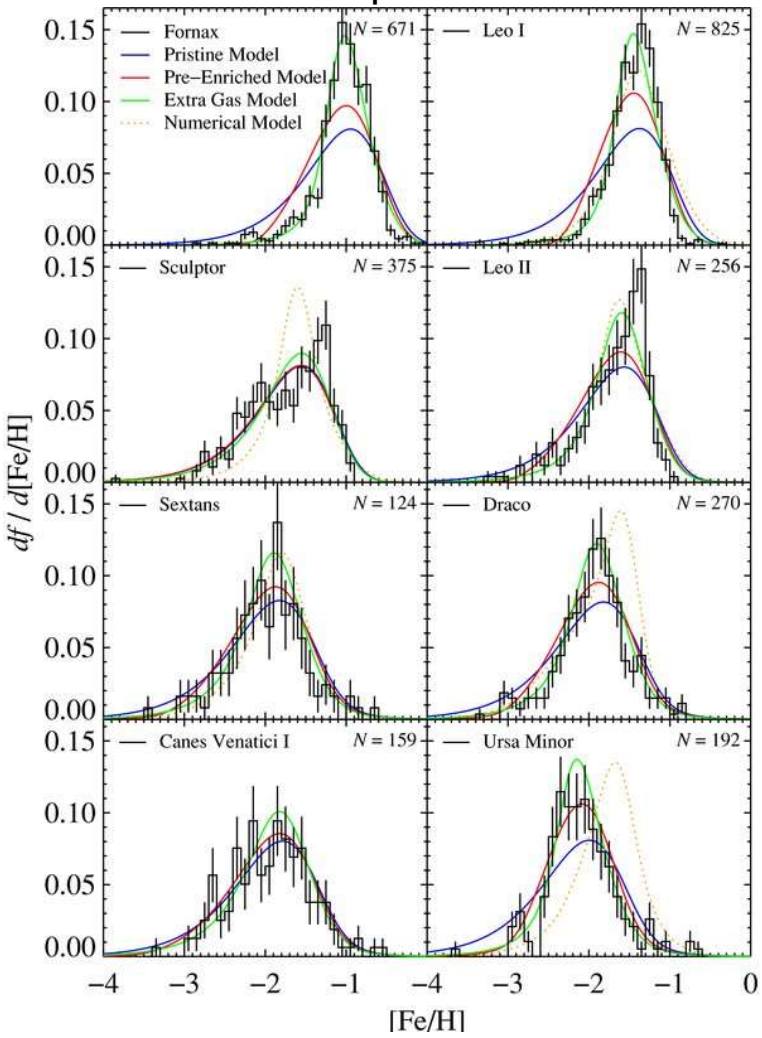

Mean [Fe/H] vs. luminosity for dSphs

Kirby et al. 2008

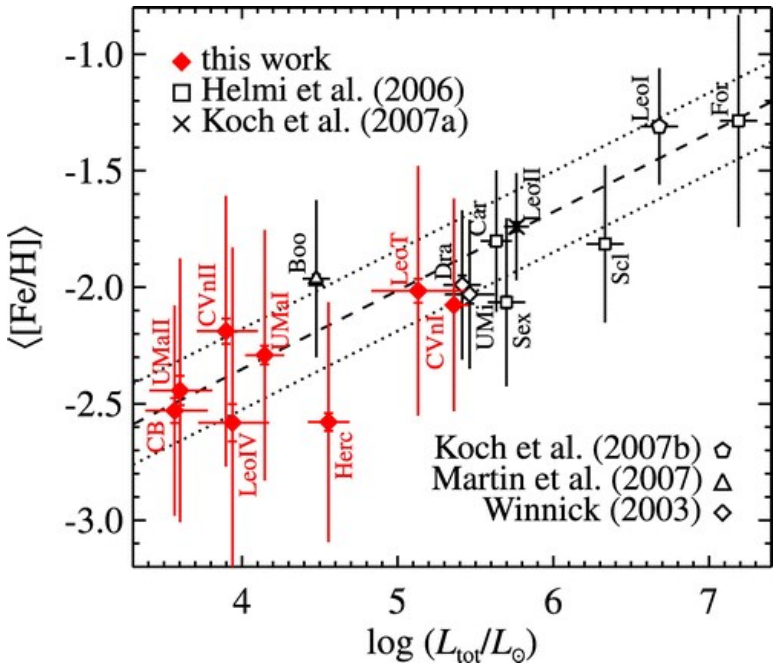

Feltzing & Chiba 2013

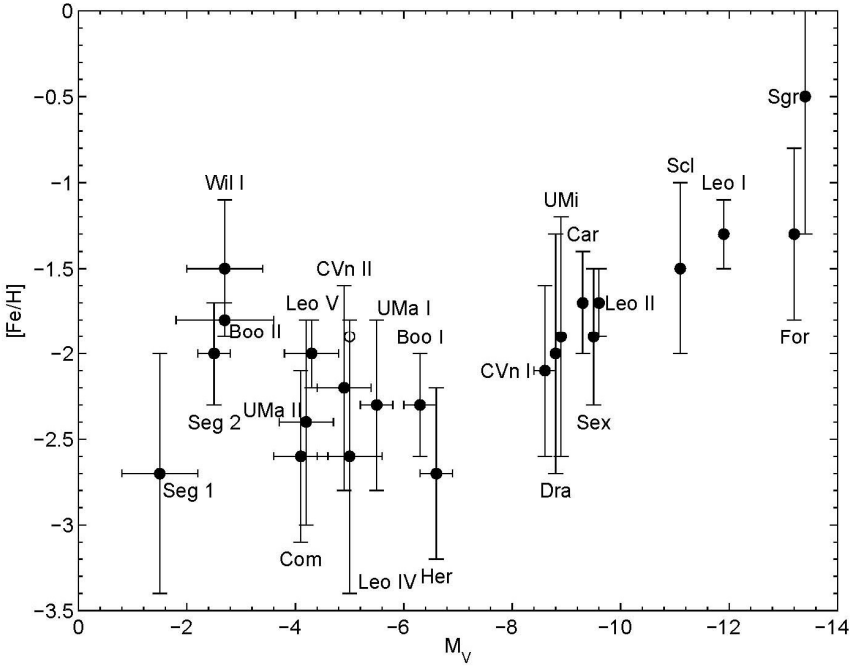

Dark matter in the MW dwarf satellites

(Mass enclosed within stellar extent ~ 4 x $10^7 M_\odot$)

Mass ratio between DM and stars

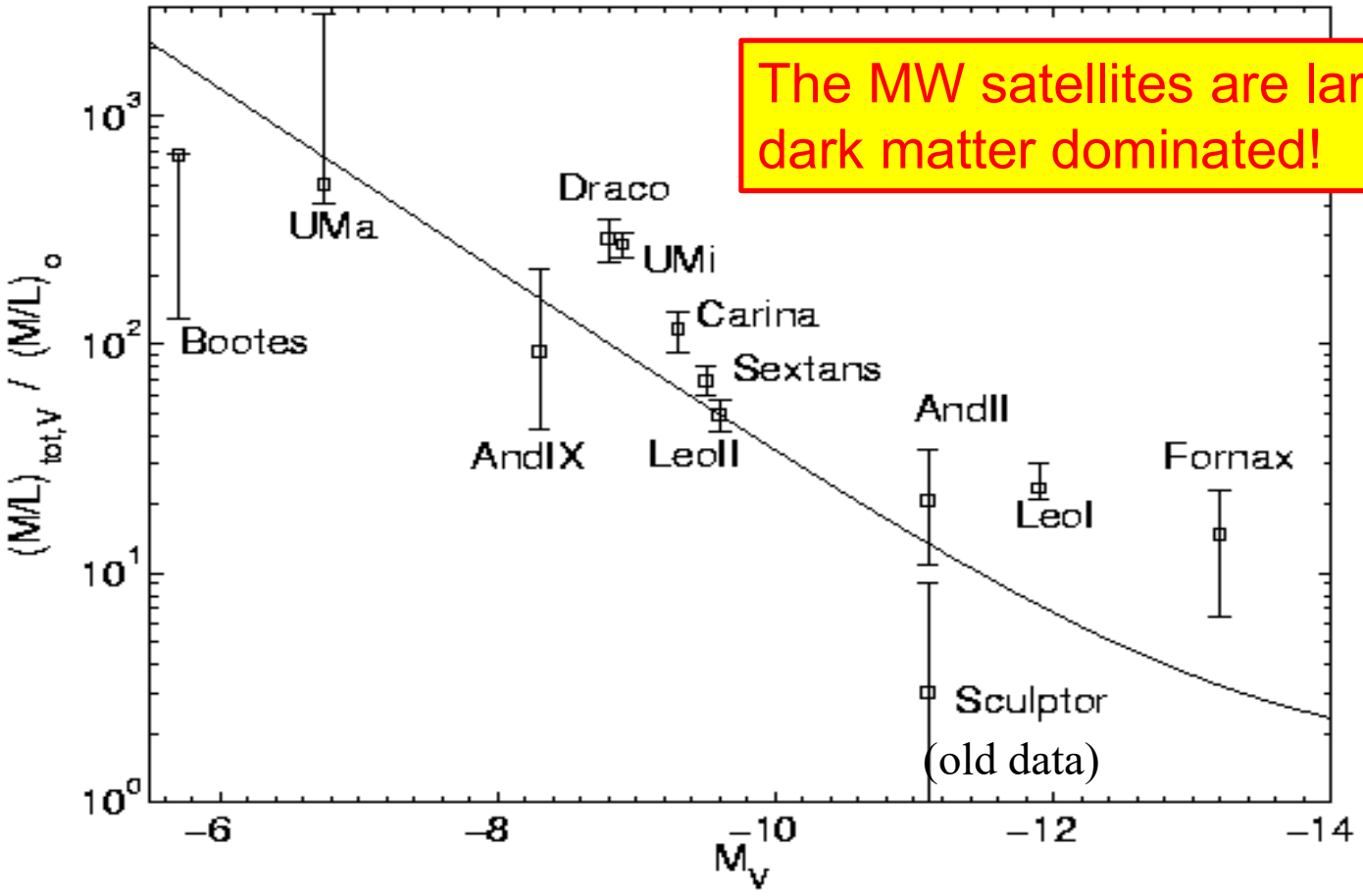

The MW satellites are largely dark matter dominated!